TECHNICAL MEMORANDUM

132

Turbulence closure applied to the parameterisation of vertical diffusion in the ECMWF model

L. Dümenil

Research Department

March 1987

European Centre for Medium-Range Weather Forecasts
Europäisches Zentrum für mittelfristige Wettervorhersage
Centre européen pour les prévisions météorologiques à moyen

CONTENTS

ABSTRACT

The parameterisation scheme for vertical diffusion in the ECMWF forecasting model is a first order closure scheme based on analytical functions (Louis et al., 1981). As an alternative scheme a simplified second order closure scheme (Mellor and Yamada, 1974) has been implemented in the model and its performance has been assessed. The scheme contains an additional prognostic equation for turbulence kinetic energy and computes diffusion coefficients that are not only Richardson number dependent as in the operational model, but depend on turbulent kinetic energy as well. For technical reasons, the model was first tested in a simpler form without taking advection of turbulent kinetic energy into account. In this version, the turbulence closure scheme performs very similarly to the operational one with slight improvements in special cases. Although the scheme partly corrects the systematically erroneous energy budget of the model by an intensified hydrological cycle, the quality of 10-day forecasts is only marginally improved. Sensitivity to the inclusion of the advection of turbulence kinetic energy suggests that these terms ought to be retained, even though no direct improvement of the forecast can be gained. The benefits that turbulence closure schemes have shown in high-resolution PBL studies is counteracted in the large-scale model by the effects of low resolution, large time-steps and the feedback from other parameterisation schemes. On the grounds of the results obtained so far, a replacement of the operational scheme by the turbulence closure scheme presented here could not be recommended. The conclusion may however become significantly different if moist processes are taken into account, and this is what is planned in future developments.

1. INTRODUCTION

When the first operational ECMWF model was designed, a first order closure was chosen for the parameterisation of vertical diffusion, because of its comparatively low computational cost. The scheme devised by Louis (1979) is based on Monin-Obukhov similarity theory using a roughness length in the surface layer and a mixing length and Richardson number dependent diffusion coefficients in all other layers. It is more sophisticated than other first order closure schemes that were used at the time in that it approximates exchange coefficients which are dependent on vertical wind shear as well as local stability by analytical functions, but at the same time simple because no explicit computation on Monin-Obukhov lengths is required.

In this study, the sensitivity of the ECMWF gridpoint model with respect to an alternative parameterisation scheme will be assessed. The level 2.5 second order closure scheme derived by Mellor and Yamada (1974) previously showed considerable improvement of skill of medium-range weather forecasts as compared to a simple first order closure scheme in the GFDL general circulation model (GFDL model physics, Miyakoda and Sirutis, 1977, Miyakoda et al. 1983).

Regarding the variables on the scale resolved by the model as mean variables and relating turbulent vertical fluxes to those, the ECMWF scheme essentially provides what is called a first order closure of the equations for turbulent quantities. Although the vertical resolution in the model is low and only a first order closure is applied, its stability dependence gives the scheme an advantage over a Prandtl-type diffusion scheme.

As assessed by Tiedtke (1981), it produces boundary layer fluxes which are in fairly good agreement with the limited number of observations available. Sensible and latent heat fluxes which enter important feedback mechanisms with other diabatic processes (e.g. via the convection scheme) are, however, insufficient to maintain the energy level of the model atmosphere on the global scale over a 10 day period.

Recent studies of high-resolution turbulence modelling have shown that vertical diffusion processes can be treated more adequately by explicitly solving the set of prognostic equations describing the evolution of

turbulence. These schemes require a large number of prognostic equations. They are called higher-order closure schemes because closure of the equations may be achieved at various levels of complexity. Second and third order closures have been devised, but in the context of parameterisation only a simplified version of a second order closure scheme such as the one given by Mellor and Yamada (1974) seems feasible. Taking into account the history of the turbulence state in terms of a prognostic equation for turbulence kinetic energy, this kind of scheme is expected to improve the representation of turbulent processes in the PBL as well as in the free atmosphere. One particular advantage of the inclusion of turbulence kinetic energy is its potential for an extension from dry vertical diffusion to the representation of cloud processes in order to cover a more complete range of the essential features of the PBL. For this, relationships between cloud properties and turbulence quantities are needed, but this will not be discussed here.

2. TURBULENCE CLOSURE

Vertical diffusion in the ECMWF gridpoint forecasting model is represented in terms of

$$\frac{\partial}{\partial z} \overline{X'w'} \qquad (1)$$

for parameters X = θ, s, u, v (potential temperature, specific humidity, horizontal wind components, respectively). The bar here denotes an averaging process over the time step and the grid length corresponding to the model resolution. X' is defined by $X = \bar{X} + X'$, where X' stands for the deviation from the mean value $\bar{X}$ and thus incorporates the random, rapid fluctuations not resolved by the model. The scale of turbulence is therefore not as narrowly defined as in turbulence theory. Further, second order correlations $\overline{X'w'}$, the so-called Reynolds stresses, are introduced by the averaging process involved in the transition from full equations to those that are solved at discrete points on the model grid. Equations for the stresses can easily be found on the basis of a set of Boussinesq equations. Due to the non-linearity of the equations, however, more unknowns are introduced than there are equations: equations for the second order correlations contain third order correlations and equations of order n contain correlations of order n+1. Solution of these sets of equations can only be achieved if additional information is provided in terms of closure assumptions.

Under the assumption that the number of equations solved prognostically increases the accuracy of the computation, the set of equations may be solved at various levels of complexity. The simplest non-trivial method is the eddy-diffusivity approach. In analogy to molecular viscosity in laminar flows that enables molecular motions to transfer momentum and heat, velocity fluctuations are assumed to exchange properties in turbulent media. With the definition of an eddy-viscosity or turbulent exchange coefficient K the equations for momentum transport read

$$\overline{u_i'u_j'} = - K \left(\frac{\partial \bar{u}_i}{\partial x_j} + \frac{\partial \bar{u}_j}{\partial x_i}\right) \qquad (2)$$

$$K = \ell^2 \left|\frac{\partial v}{\partial z}\right| \qquad (3)$$

In this widely used concept, a first order closure is given by relating second order moments to mean variables only using Prandtl's mixing-length theory.

Although this approach proves quite useful in the description of simple flows, a more general and sophisticated method is desirable. In order to adequately describe the state of turbulence at a particular point it may be necessary to take into account sources and sinks at other points of the flow or at an earlier time. For this purpose, prognostic equations for the stresses are derived. The third order correlations which occur then are modelled according to assumptions given by turbulence theory so that they depend on second order correlations and mean values only (second order closure). A standard set of assumptions has been compiled (described in Deardorff (1973) and Donaldson (1973)) and developed, thus enabling the description of turbulent processes to a higher degree of accuracy by a second order closure scheme (Deardorff, 1972; Mellor, 1973; Wyngaard and Coté, 1974; Sommeria, 1976). André et al. (1976) relate fourth order correlations to those of lower order in a third order scheme for use in a one-column boundary layer model of high vertical resolution.

The numerical solution of a full second order closure scheme in three dimensions requires a large computational effort (Deardorff, 1974). In search for a simplification as far as atmospheric turbulence in the Planetary Boundary Layer is concerned, Mellor and Yamada (1974 and Corrigendum by Lipps, 1977) examined the information contents of a full second order closure scheme (10 additional prognostic equations for second order quantities). Under the assumption of isotropy of boundary layer turbulence, a hierarchy of simplified sets of equations was derived and their performance compared. As a compromise between accuracy of the PBL simulation and computational requirements, only one additional prognostic variable, turbulence kinetic energy (TKE), was retained.

From the remaining set of diagnostic equations, diffusion coefficients K_M and K_H for momentum and heat, respectively, are derived. These are now depending on mean variables and TKE, a second order quantity.

In this study, the same set of equations is used, except for the correction given by Lipps (1977). Comparison here will be with the stability and slower dependent scheme by Louis (1979). Level 2.5 model with a diagnostic ℓ has been implemented in the GFDL general circulation model (Miyakoda and Sirutis, 1977), where a significant improvement was achieved over the simple

parameterisation of boundary layer processes by the first order closure scheme using a mixing-length with $K = \ell^2 \left| \frac{\partial v}{\partial z} \right|$ (GFDL physics, 1965).

3. IMPLEMENTATION OF A TURBULENCE CLOSURE SCHEME INTO THE ECMWF GRID POINT MODEL

In the gridpoint model, which was used in this study, the model equations for T, s, u, and v include the source terms due to radiation and unresolved physical processes like vertical diffusion and deep convection (Appendix A). These processes have to be parameterised. The parameterisation scheme for vertical diffusion deals with sub-scale turbulent fluxes in a moist atmosphere, where no phase changes occur (Tiedtke et al., 1979). Deep convection is treated separately by the Kuo-convection scheme. Enhanced vertical mixing induced by shallow convection was not accounted for at the time this work was initiated.

In the present study, the stability dependent vertical diffusion scheme that has been used in the operational ECMWF forecasting model since 1979, is replaced by an economical turbulence closure scheme. The scheme is less sophisticated than a full second order closure scheme in that it only requires one additional prognostic variable for TKE. A second variable such as a prognostic length scale (Rotta, 1951, Yamada and Mellor, 1979) or $\overline{\theta'^2}$ (Mellor and Yamada, 1974) cannot be easily accomodated in a global numerical forecasting model, where computer storage and computation time are an important constraint.

Turbulent kinetic energy, hereafter denoted q^2, is determined according to the following evolution equation:

$$\frac{D}{Dt}\left(\frac{q^2}{2}\right) = \frac{\partial}{\partial t}\left[\frac{5}{3} C_1 \ell q \frac{\partial}{\partial z}\left(\frac{q^2}{2}\right)\right] - \overline{u'w'}\frac{\partial \bar{u}}{\partial z} - \overline{v'w'}\frac{\partial \bar{v}}{\partial z} + \beta g \overline{w'\theta'_v} - \frac{1}{B_1 \ell} q^3 \qquad (4)$$

$$\text{with} \quad \ell = \frac{kz}{1+\frac{kz}{\ell_o}} \qquad \ell_o = 0.1 \frac{\int_o^z q\, z\, dz}{\int_o^z q\, dz} \qquad (5)$$

where ℓ is a characteristic length scale defined following Blackadar (1962) k is the von Karman constant and C_1 and B_1 empirical constants (Mellor and Yamada, 1974)

The equation for turbulent kinetic energy TKE accounts for its production by the mean shear stress and production or destruction by buoyancy as well as diffusion and dissipation. Advection has not been included in the one-dimensonal tests and most of the global integrations, because it was assumed that on the time and space scale of the model its effect would only be small in comparison to production terms. This will be discussed in connection with sensitivity studies.

Here, the ℓ expression by Blackadar (1962) (Eq.5) was chosen on the grounds of simplicity and because it has been used successfully in the operational model with a fixed asymptotic mixing length ℓ_o. The same equation (5) has also been chosen in the first applications of the turbulence closure scheme to boundary layer modelling (Mellor and Yamada, 1974). ℓ becomes a function of the barycentre of turbulence which is found in the PBL. If this formula is applied to turbulence in the free atmosphere as it is done in the ECMWF model, a distinct disadvantage of this formula becomes evident: ℓ is essentially non-local and turbulence may not be well represented at the higher levels of the model (see section 4.).

Using a finite difference scheme, the TKE equation (without advection terms) is integrated in time in two parts. Firstly, production/dissipation are added,

$$q_*^{2\ t+1} = q^{2\ t-1} + 2\Delta t\ (P-D) \qquad (6)$$

secondly, the intermediate value $q^2{}_*T+1$ enters the diffusion equation

$$q^{2\ t+1} = q_*^{2\ t+1} + 2\Delta t\ Df \qquad (7)$$

This is solved implicitly with boundary conditions $q^2 = 0$ at the top of the model and $q^2 = B_1^{2/3} u_*^2$ at the lowest model level (about 30 m) following the method by Richtmeyer and Morton (1967). q^2 is then used to establish diffusion coefficients K_M and K_H required for the solution of the diffusion equations for T, s, u, and v by the same method.

In the surface layer, Monin-Obukhov similarity is used as in the operational model. For all other model levels, the following equations are used:

$$\overline{w'u'} = - K_M \frac{\partial \bar{u}}{\partial z}$$

$$\overline{w'v'} = - K_M \frac{\partial \bar{v}}{\partial z}$$

$$\overline{w'\theta'} = - K_H \frac{\partial \bar{\theta}}{\partial z} \qquad (8)$$

$$\overline{w's'} = - K_H \frac{\partial \bar{s}}{\partial z}$$

K_M and K_H are now defined as

$$K_M = \frac{\ell_1\{(1-3c)q^5+3\ell_2[\Lambda_2-3\ell_2)q^3+3(4\ell_1+\Lambda_2)cq^3]\beta g\frac{\partial\theta}{\partial z}\}}{q^4+6\ell_1^2q^2\left|\frac{\partial \bar{v}}{\partial z}\right|-3\ell_1\ell_2\beta g\frac{\partial\bar{\theta}}{\partial z}[6\ell_1(\Lambda_2-3\ell_2)\left|\frac{\partial \bar{v}}{\partial z}\right|+(7+\Lambda_2/\ell_1)q^2-9\ell_2(4\ell_1+\Lambda_2)\beta g\frac{\partial\bar{\theta}}{\partial z}}$$

$$K_H = \frac{\ell_2[q^3-6\ell_1K_M\left|\frac{\partial \bar{v}}{\partial z}\right|]}{q^2-3\ell_2(4\ell_1+\Lambda_2)\beta g\frac{\partial\bar{\theta}}{\partial z}} \qquad c = 0.056 \qquad (9)$$

K_M and K_H vary slightly from the coefficients used by Miyakoda and Sirutis (1977) in that the correction to the equations proposed by Lipps (1977) has been applied.

The following empirically derived constants were found using boundary layer approximations (Mellor and Yamada, 1974)

$$(\ell_1, \ell_2, \Lambda_1, \Lambda_2) = \ell\ (A_1, A_2, B_1, B_2)$$
$$= \ell\ (0.78,\ 0.79,\ 15.0,\ 8.0) \qquad (10)$$

These constants have later been amended as more boundary layer data became available. The above-mentioned set has, however, been used in all integrations of this study, since the model results in this particular application were not sensitive to the proposed changes in these constants. The overall choice of these variables by which a distinction is made between the length scales associated with mixing and dissipation, defines the value of the critical flux Richardson number at which turbulence vanishes, but that has not changed with the above mentioned modifications. In boundary layer studies it is reasonable to have $R_{i,cr} = 0.25$ in agreement with observations. The constants in Eq. 9 have been chosen in order to achieve such a turbulence cut-off at $R_{i,cr} = 0.21$ (Mellor and Yamada, 1974). Application of the scheme to the free atmosphere, which the full second order equations do not exclude, is however restricted. Turbulence occuring at higher Richardson numbers, e.g. clear air turbulence near the tropopause, cannot be represented by the scheme - but cannot be expected to be resolved in the model either. The operational diffusion scheme allows a wider range of Richardson numbers up to $R_{i,cr} = 1$.

The diffusion coefficients in Eq.(9 a,b) differ from those in the operational scheme as they are related to TKE as well as vertical shear and stability. In contrast to the operational scheme, the coefficient for heat transfer allows for counter-gradient fluxes explicitly, an effect which is built into the second moment equations and is retained after the simplifications. The main problem in the application of the scheme stems from the simplification of the equations under the assumption of isotropy. Under certain circumstances, the diffusion coefficients may well become infinite. During the period of creation of turbulence in unstable conditions while it is far from its equilibrium value, the stability term in the denominator of (9) may become dominant and thus $K_{M,H}$ have singularities. In order to keep the scheme stable, the diffusion coefficients are artificially limited by the value 10^4. In view of the problems encountered with such singularities, Helfand and Labraga (1983) chose a diagnostic equation for TKE in the parameterization scheme of the GLAS model.

Due to the various feedback mechanisms between parameters q^2, ℓ and $K_{M,H}$ and the influence of the large time-step of the model, which is much larger than the characteristic time scale of turbulence, a careful initialisation of q^2 is required. At the first time-step q^2 is therefore computed from the equilibrium condition

$$0 = - \overline{u'w'} \frac{\partial \bar{u}}{\partial z} - \overline{w'v'} \frac{\partial \bar{v}}{\partial z} + \beta g \, \overline{w'\theta_v'} - \frac{1}{B_1 \ell} q^3 \qquad (11)$$

where diffusion coefficients are taken from the analytical functions of the ECMWF diffusion scheme. From this initial state q^2 quickly adjusts as it is clearly dominated by production and dissipation terms.

The resulting full parameterisation scheme requires more computational effort than the ECMWF scheme, because an additional equation has to be solved. This further increases with the addition of advection terms. For each timestep the additional cost is by about 10%.

4. DISCUSSION OF RESULTS

For testing purposes, the parameterisation scheme outlined in the previous section has first been implemented into the one-column version of the ECMWF grid-point model. Initialised with observational data, this model provides an inexpensive testing facility. Advection terms may either be prescribed or neglected if appropriate. In order to study the effects of dry turbulent mixing in the absence of clouds two data sets were available. After testing in the one-dimensional case the scheme has then been incorporated into the global model. Global integrations normally focus on the performance of the model in terms of forecasting skill, but also the time evolution of the flow or the thermodynamic structure in a particular area of the globe can be studied. Finally, confidence in the performance of a special model configuration may be gained by extending integrations to up to 50 days and studying the model climate.

4.1 One-dimensional tests

4.1.1 Leipzig data set

Wind data gathered by Mildner (1932) at Leipzig represent a steady, uniform wind field under slightly stable conditions. The data which has been reanalysed by Lettau (1950) on the assumption that shear stress and vertical wind vector are parallel in the boundary layer is the so-called 'Leipzig wind profile'. It is an example of an equilibrium boundary layer as it is found in the warm sector of a well-developed cyclone. As baroclinic waves are controlled by energy transports and dissipation, it is justified to investigate these features by the aid of an idealised data set.

The integration of the horizontal wind components is governed by

$$\frac{\partial \vec{v}}{\partial t} = f \quad K \times (\vec{v}_g - \vec{v}) \qquad (12)$$

with $f = 1.14\ 10^{-4}\ s^{-1}$ at Leipzig. T and s fields are kept constant during the integration assuming a lapse rate of 0.65 K/100m constant with height. The roughness length z_o is specified as $z_o = 0.07$ m and $|\vec{v}_g| = 17.5\ m\ s^{-1}$ is reached at the fourth model level.

Tiedtke (1981) has assessed the performance of the operational ECMWF diffusion scheme concerning the transport of momentum in the vertical. Both the ECMWF and turbulence closure scheme (TC) adjust quickly to equilibrium

values. Compared with the observations, the equilibrium profiles, however, exhibit the same deficiencies. At the lowest model levels the flow is stronger by up to 2-3 m s^{-1} than observed (Fig. 1). For TC this is less pronounced, because a larger exchange coefficient (Fig. 2) produces a larger surface stress.

Lettau (1950)	0.54 N m^{-2}
Carson and Smith (1973)	0.46 N m^{-2}
ECMWF scheme	0.50 N m^{-2}
TC scheme	0.57 N m^{-2}

Momentum flux components t_x and t_y in Fig. 3 show the low resolution representation of turbulent fluxes in the ECMWF model against the background of high-resolution observations. The agreement between the two is very good and it becomes clear that the TC successfully drains energy from above to be dissipated near the surface.

The calculation of the diffusion coefficients in the TC scheme depends on interactive parameters, ℓ and q^2. In the TC parameterisation, ℓ reaches an asymptotic value of 60 m in the PBL as compared to 30 m as derived from the data (Carson and Smith, 1973, 1977). Exchange coefficients based on identical profiles are found to be considerably larger. In neutral to slightly stable conditions the momentum exchange is therefore increased as compared to the ECMWF scheme.

The idealised case of the Leipzig data shows that the currently operational ECMWF diffusion scheme gives a good representation of the essential processes in the bulk of the boundary layer in near-neutral stability conditions, although the model's vertical resolution is very low. The difference between the two parameterisation schemes quickly leads to different equilibrium states. The TC allows increased momentum transports and more energy to be dissipated in the surface layer. Although this is a desirable feature in principle, the decision on which scheme performs better is difficult in this case, because the TC scheme overestimates the surface stress by the same amount by which the ECMWF scheme underestimates it.

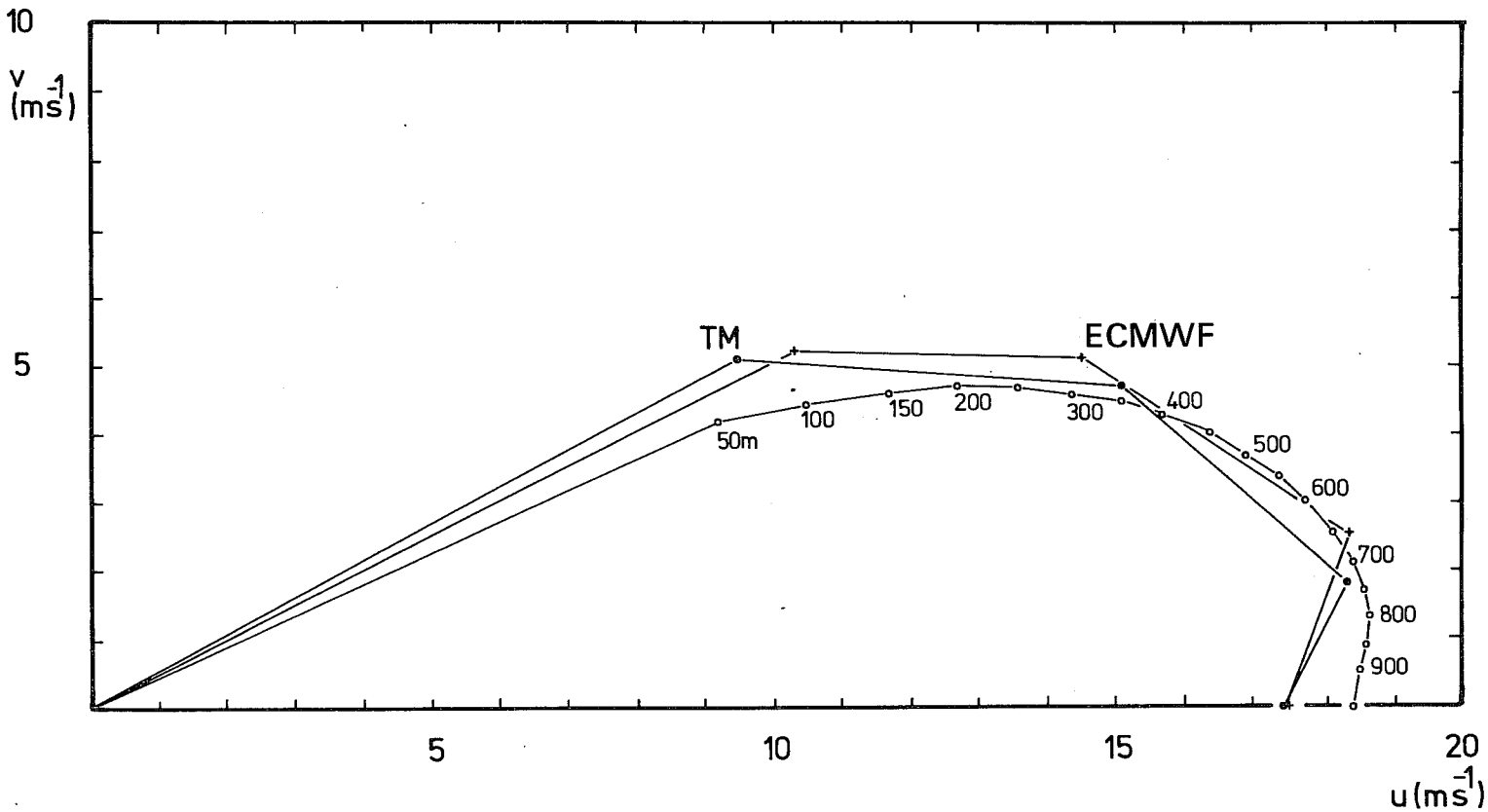

Fig. 1 Leipzig wind profile. u- and v- wind components calculated by Carson and Smith (1973) -.- and values at model levels (34, 289, 759 and 1415 m, where $v=v_g$) for the operational scheme (ECMWF) and the turbulence closure scheme (TM).

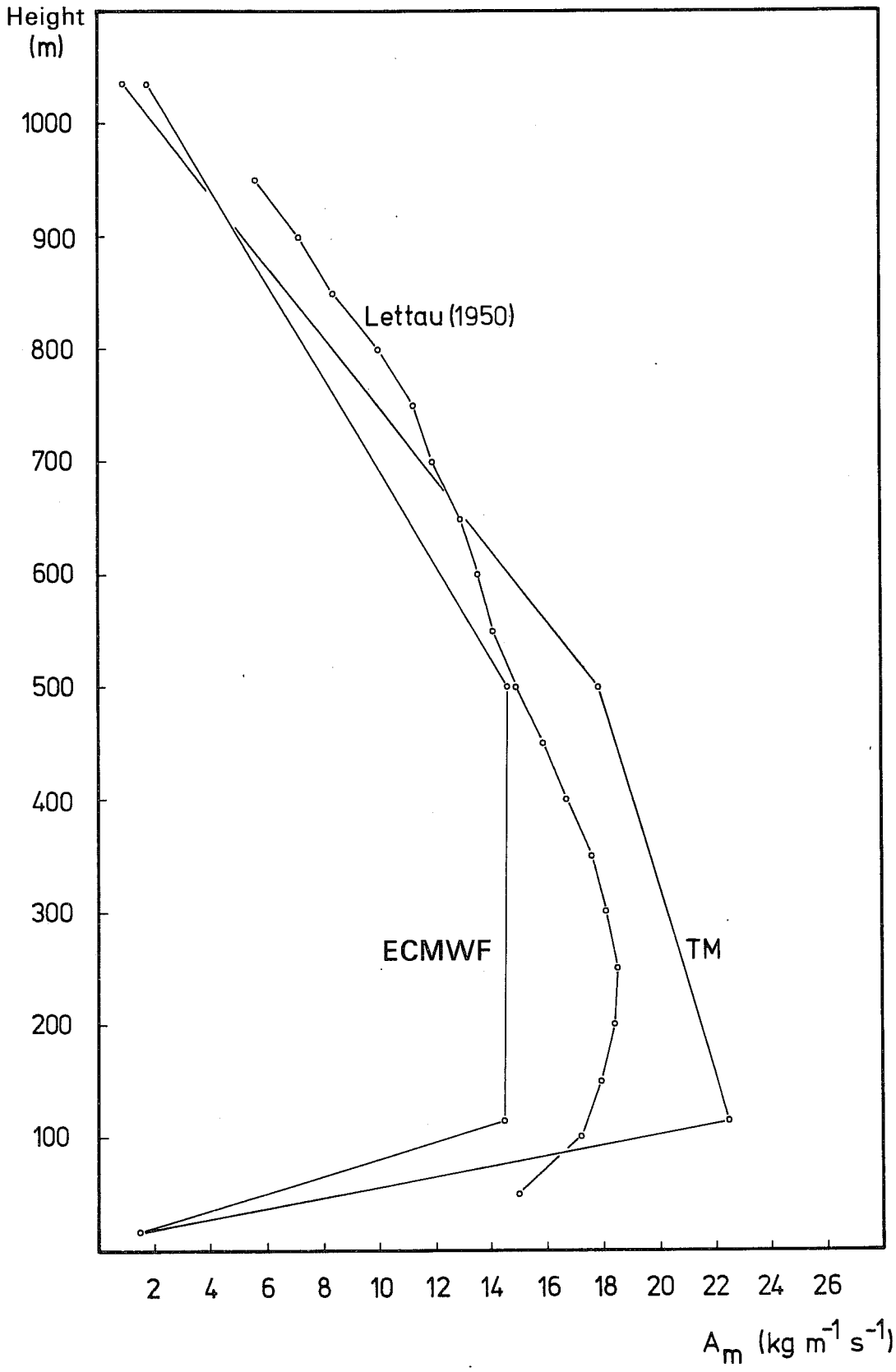

Fig. 2 Leipzig profile. Comparison of exchange coefficients calculated by Lettau (1950) -.-, for the operational scheme (ECMWF) and the turbulence closure scheme (TM).

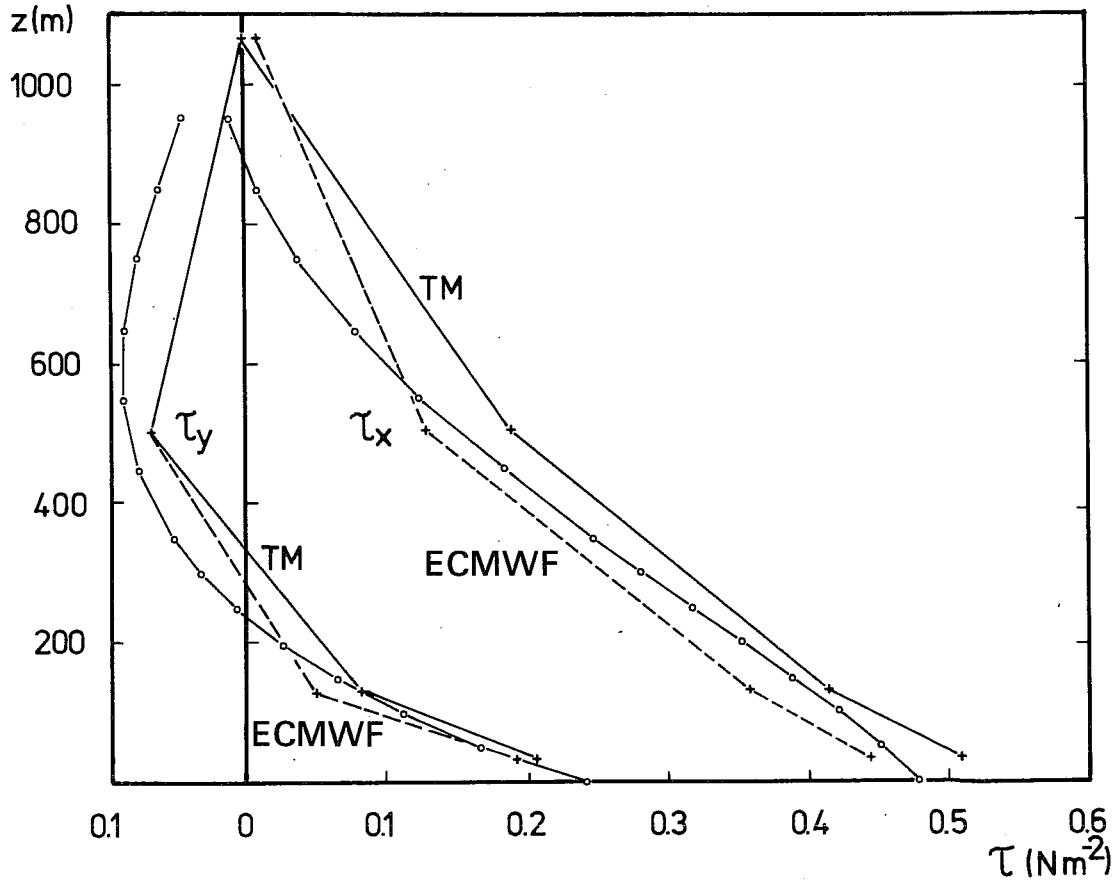

Fig. 3 Leipzig profile. Surface stress τ as given by the operational and turbulence closure scheme, respectively and its components in the x- and y- directions τ_x and τ_y. -.- values given by Carson and Smith (1977).

4.1.2 Wangara dataset

The Wangara dataset (Clarke et al., 1971) was obtained at Hay, Australia, in the summer of 1967 and consists of radiosonde ascents and wind profiles for the boundary layer at 3-hourly intervals. It has been the basis for several high-resolution studies of the PBL using second order closure schemes (e.g. Mellor and Yamada, 1974, Therry and Lacarrère,1983, Mailhot and Benoit, 1982, and Deardorff, 1974, for a detailed three-dimensional numerical simulation).

In contrast to the previous example, this case study is dominated by dry convective processes, where turbulence is generated by buoyancy. The one-dimensional model is initialised by the profiles of T, s, u and v at day 33 (16 August 1967, 00 local time). The simulation recreates a cloud-free situation where frontal effects and advection are assumed to be negligible. The diurnal variation of radiation is imposed by increasing the frequency of the radiation computation in the model and results in the following: after sunrise a mixing layer develops in the four lowest layers of the model with a maximum of turbulence in the early afternoon. After sunset turbulence vanishes but the well-mixed layer remains intact, although decoupled from the surface layer. The surface temperature quickly adapts to the radiative cooling.

The representation of this buoyancy driven boundary layer depends strongly on the choice of surface parameters. The interactive soil parameterisation allows the energy input at a moist surface to be used for evaporation and therefore the latent heat flux is favoured if the soil is wet. In order to emphasize the flux of sensible heat and allow for an appropriate diurnal variation of surface temperature the ground moisture contents has been set to a fairly low value (5 % of the saturation value). Clarke et al. (1971) do not mention any specific values for this quantity.

Under these conditions the ECMWF and TC model integrations over 24 hours represent a full diurnal cycle of turbulent exchanges. During the phase of creation of turbulence parameters q^2, ℓ, K_M, and K_H are subject to multiple feedbacks. q^2 remains small until suddenly - behaving like a step-function rather than gradually increasing - it becomes sufficiently large to make the whole layer turbulent. This then produces considerable changes in the T and s

profiles (Figs. 4-6). After 18 hours of integration both the ECMWF and TC scheme have created a mixed layer with similar properties. θ is found to be 285.5 K at all the model levels up to 850 mb for the TC scheme and 285.6 K for the ECMWF scheme. Fig. 6 reveals how these values compare with observations. After local noon, the disagreement between observations and model results is 2.5 K over the whole mixed layer. This is due to insuffient mixing with warm air from above (Manton,1983) and too little sensible heat flux through the interface with the surface layer at about 30 m (lowest model level). Here, q^2 is computed as a function of u_* which is based on Monin-Obukhov similarity theory underestimating the flux through this level. As a consequence, the surface layer completely decouples from the rest of the PBL. Although the surface temperature undergoes a large daily variation under the influence of the diurnal cycle of solar radiation (Fig. 7), the induced heat content of the surface layer (Fig. 6) is not communicated to higher levels. The problem of lower heat contents of the well-mixed layer cannot be alleviated by the prescription of advection effects nor a different prescription of the soil conditions. The aspect of low vertical resolution in the ECMWF model has been investigated by Manton (1983). There are, however, indications that the interaction between the PBL-, surface layer- and surface temperature parameterisations is unbalanced, as studies where the surface temperature is not predicted achieve better agreement.

After the radiation input that drives the PBL has ceased, turbulence vanishes abruptly, leaving a well-mixed layer behind. Although the diffusion coefficients are still large, they do no longer cause effective changes in T and s. The Wangara dataset only provides a transition from unstable stratification during the day to stable stratification at night in the surface layer where Monin-Obukhov similarity theory is applied.

Summarizing, it can be said that the ECMWF first order and the turbulence closure schemes achieve similar results for a case of buoyancy generated turbulence. Due to the large time-step and large model slabs, turbulence sets in abruptly rather than representing a slow build-up of the mixed layer. The combination of the schemes with the forecast of surface layer and ground

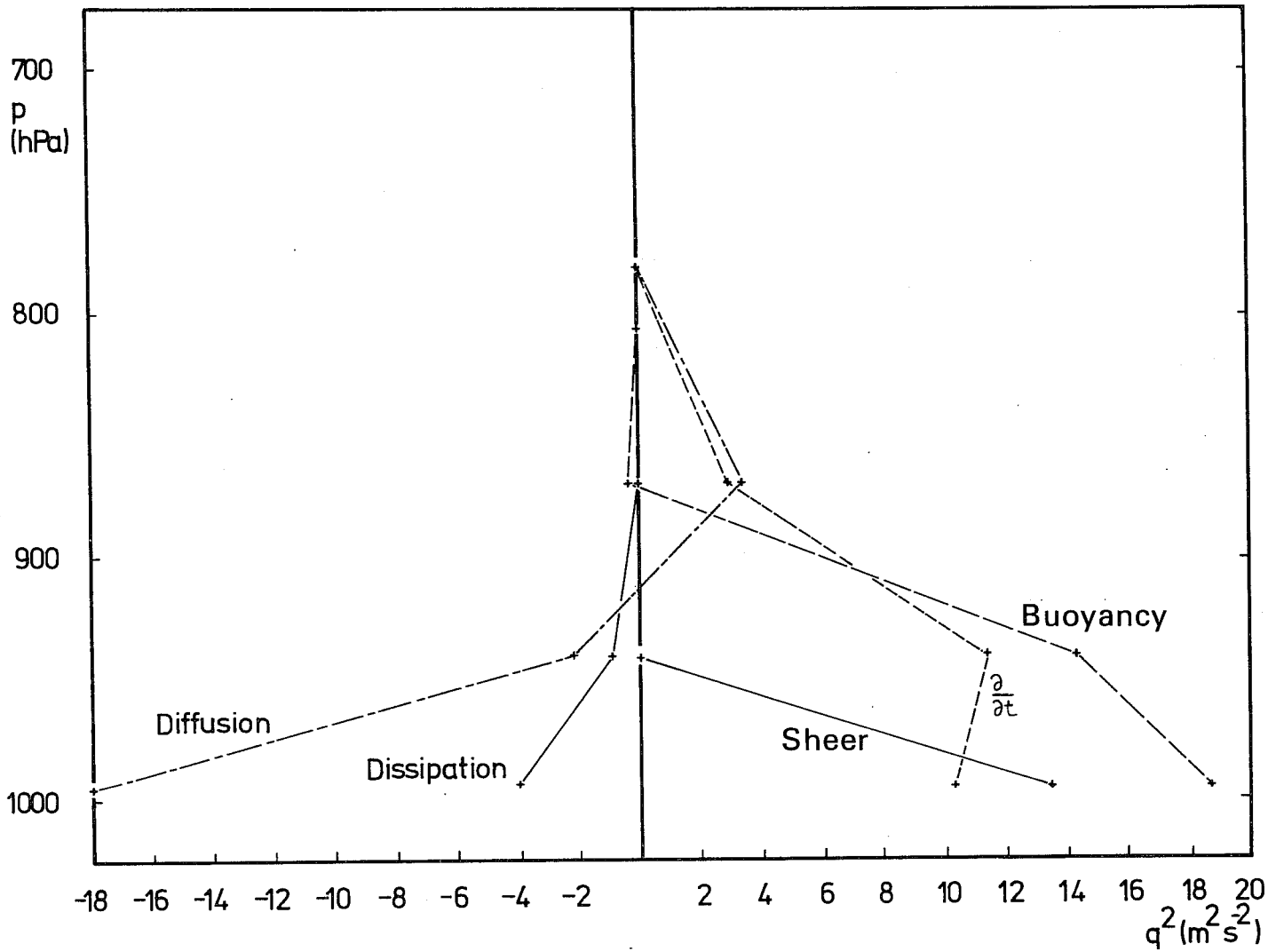

Fig. 4 Wangara. Components of the equation for q^2 at 13.7 hours (mixing layer).

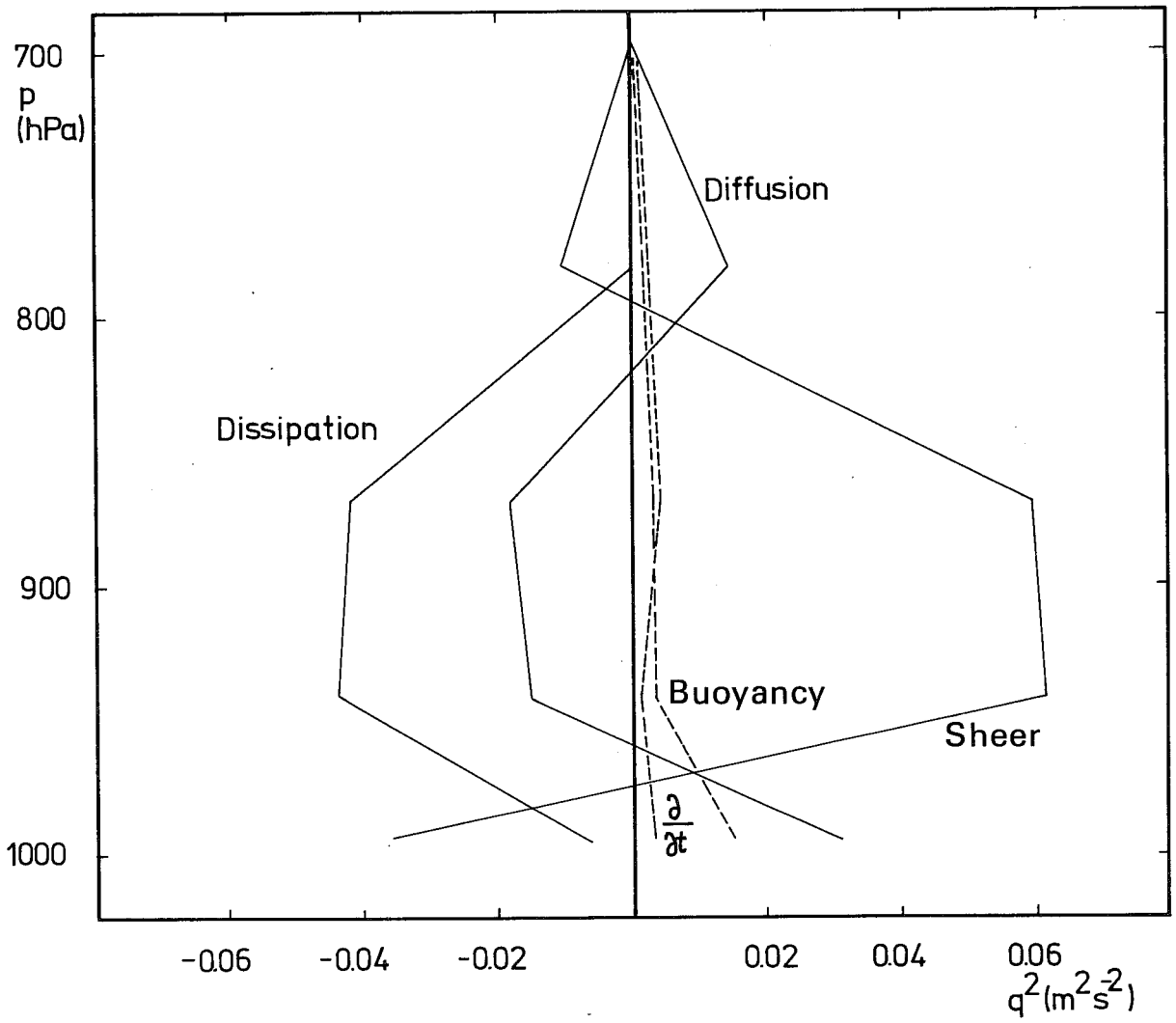

Fig. 5 As Fig. 4 but at 21.7 hrs (well mixed layer).

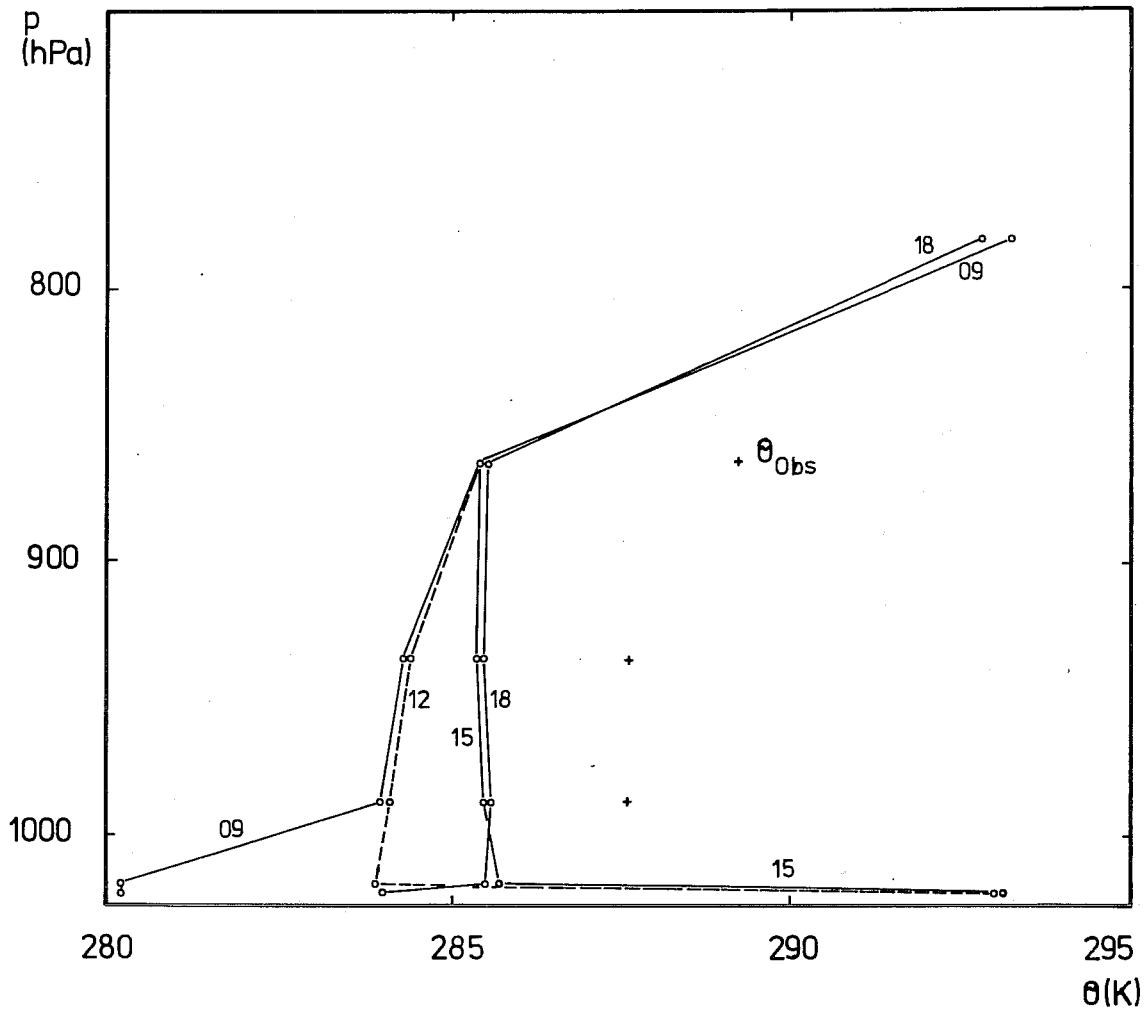

Fig. 6 Wangara. θ-profiles within the PBL during a diurnal cycle Integration with the turbulence closure scheme. θ observed at levels corresponding to model levels denoted by +.

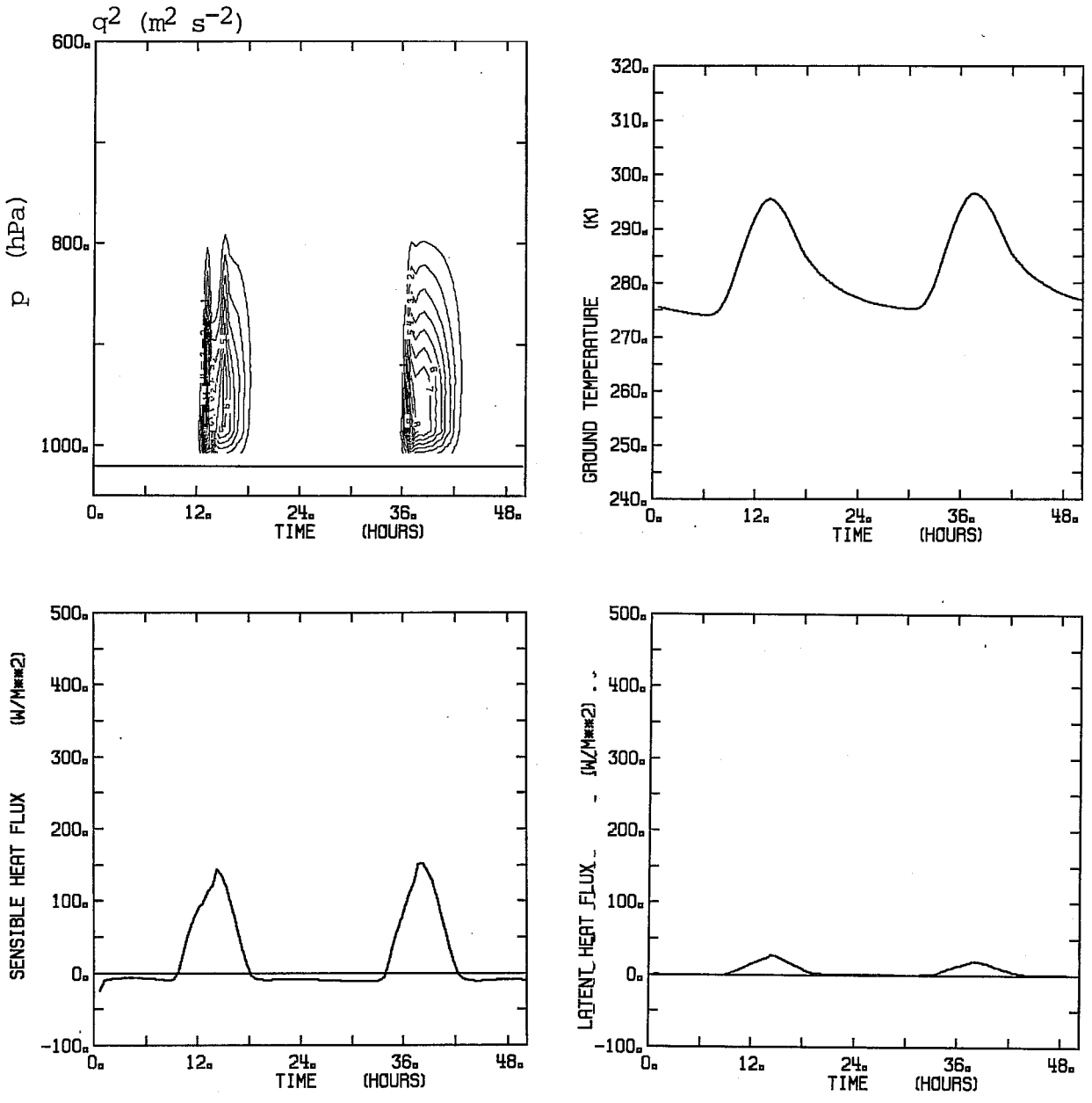

Fig. 7 Wangara. Diurnal variation of the turbulence kinetic energy (top left), surface temperature (top right), sensible heat flux (bottom left), and latent heat flux (bottom right).

parameters in the ECMWF forecasting model seems to have an adverse effect on the performance of both schemes.

4.2 Global integrations

4.2.1 Air mass transformation

The case of a cold air outbreak over the East China Sea can be studied in a 24 hour integration initialised from a FGGE global analysis (18/1/1979 12 Z). During a relatively short period a cold dry continental air mass is advected over the sea with a fast warming and moistening. A radiosonde ascent at Naze (28.1°N, 129°E) is available for comparison of model results with observations. Climatological features are similar to the well-documented observations during AMTEX 74 (Ninomiya and Akiyama, 1976).

The performance of the ECMWF model in this particular case has been assessed by Tiedtke (1981) for an integration where the Kuo deep convection scheme has been replaced by the Arakawa-Schubert convection scheme. The representation of the air mass transformation in the ECMWF model is in good agreement with observations. The strong cooling and drying due to advection is compensated for by turbulent fluxes of sensible and latent heat at lower levels and by deep and large-scale convection above 850 mb. Similar results are obtained if the vertical diffusion scheme is replaced by the turbulence closure scheme (and combined with the Kuo scheme). The profiles of heating and moistening over the 24 hour period are compared in Figs. 8 and 9. Eventually the balancing by turbulent fluxes establishes the thermodynamic structure as shown in Fig. 10. Both the ECMWF and TC scheme misplace the height of the inversion as compared to observations by 50 mb. This is essentially a resolution problem. The TC scheme, however, creates an improved stronger gradient because cooling occurs at the 850 mb level as a consequence of the counter-gradient flux which the operational scheme does not include. The moisture flux does not extend beyond 800 mb and this layer quickly becomes saturated as no mixing at the top of the PBL occurs. The ECMWF model transports a smaller amount of moisture upwards.

Both schemes equally suffer from the lack of a representation of shallow convection. In the absence of advection both the shear and buoyancy production terms are balancing the dissipation of TKE. Again the dominant

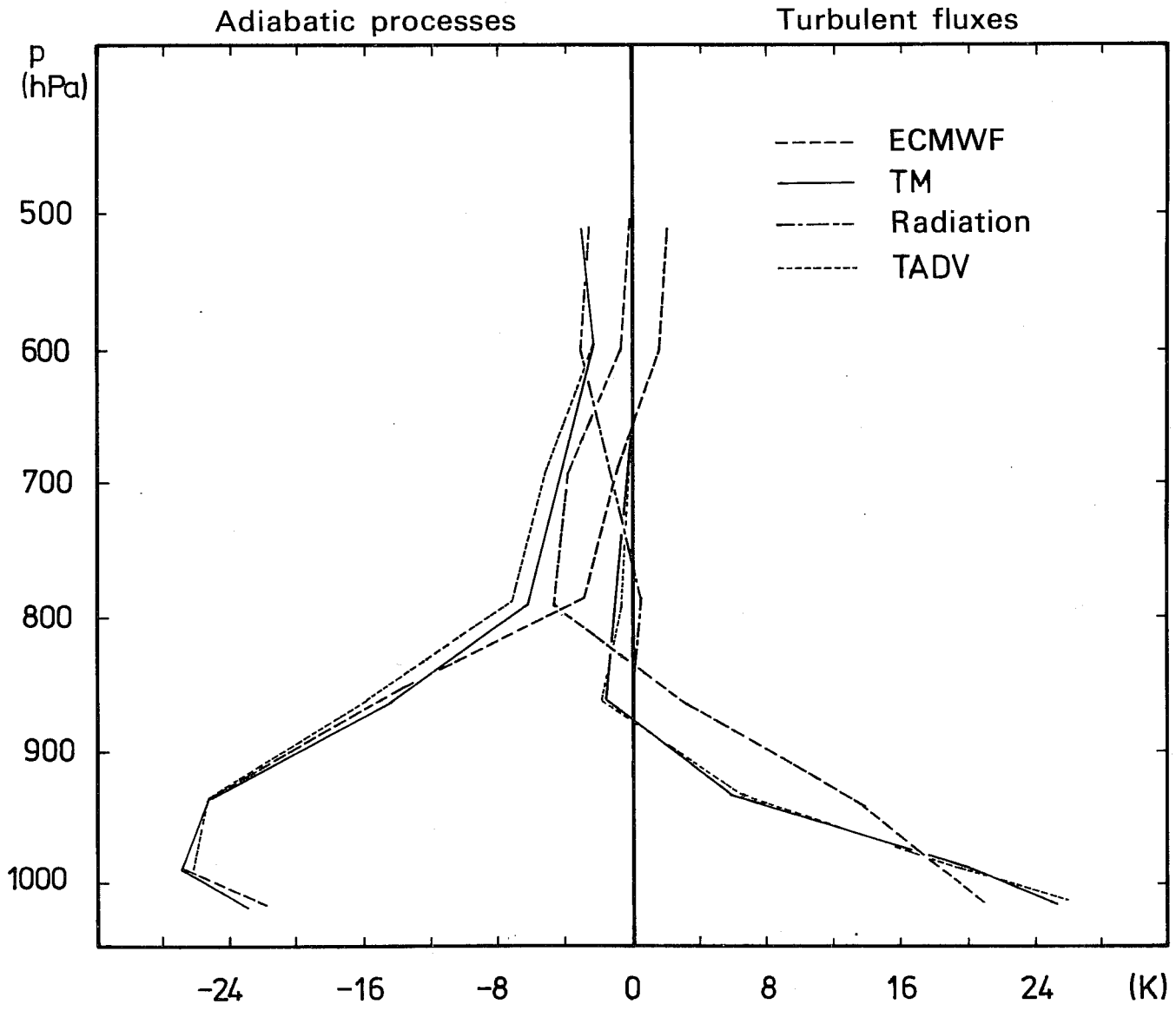

Fig. 8 Cold air outbreak over the East China Sea. Integration from the FGGE analysis of 18/1/1979 12Z. Net heating over a 24 hr period due to adiabatic and diabatic processes, respectively.

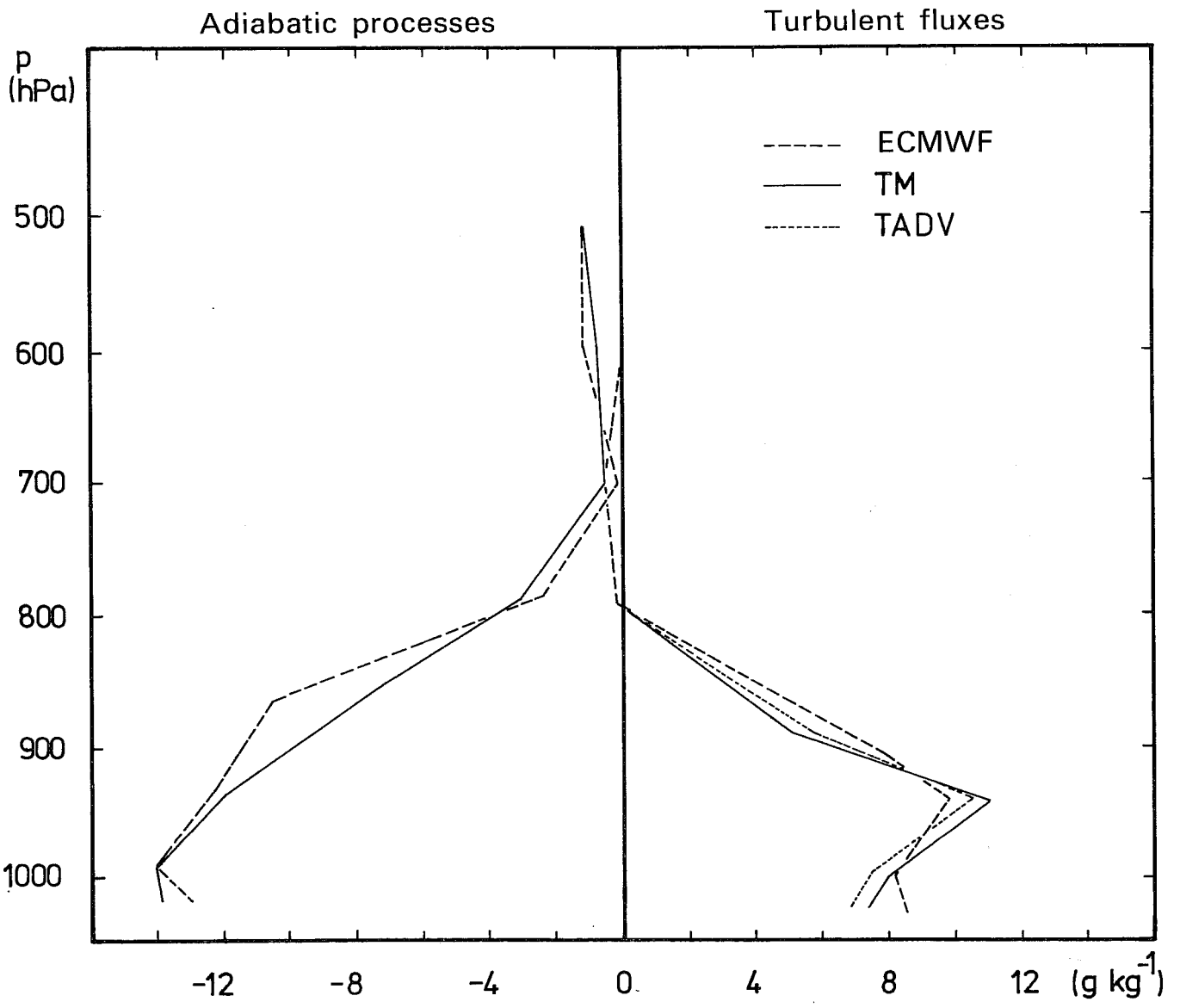

Fig. 9 As Fig. 8 but for moistening.

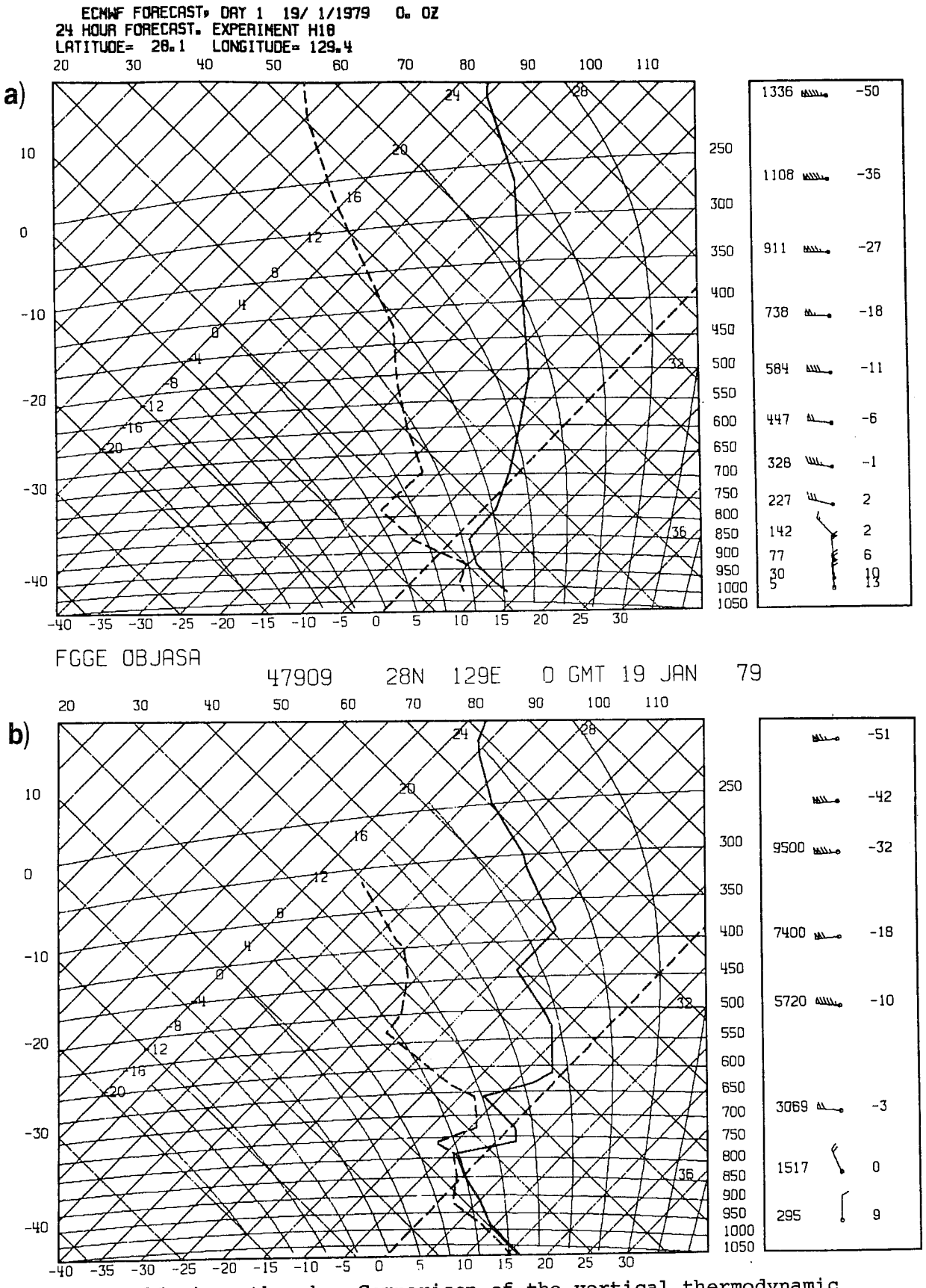

Fig. 10 Cold air outbreak. Comparison of the vertical thermodynamic structure over 24 hours of integration.
a) nearest grid-point operational model.
b) radiosonde ascent at Naze.

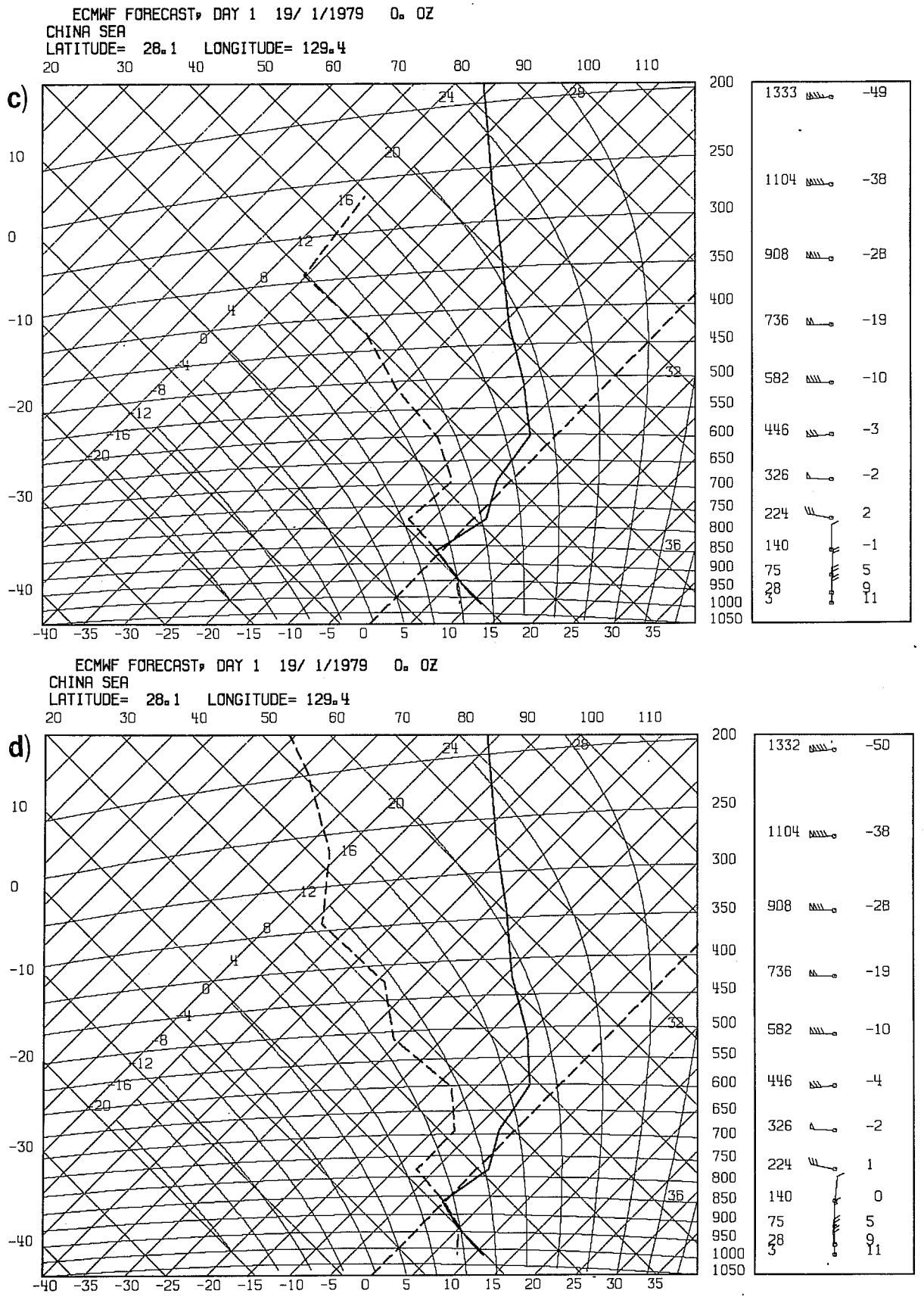

Fig. 10 c) nearest grid-point turbulence closure scheme no advection of TKE
d) with advection of TKE.

production terms enable a quick adjustment of TKE to the situation independent of the initial conditions, the maximum amount of TKE is already reached at 12 hours into the integration. The effect of advection and other parameters on the performance of the scheme will be discussed in the following section.

4.2.2 Sensitivity studies

a) Use of θ_v

The formulation of diffusion coefficients K_M ad K_H was chosen to be a function of θ_v, the virtual potential temperature, rather than θ as a consequence of the application of the scheme to a moist atmosphere, where buoyancy is related to θ_v. This formula seems to be beneficial as it favours the latent heat flux which in turn improves the input to the deep convection parameterisation that depends on moisture convergence. The influence of moisture on the amount of turbulence is illustrated by the following example.

The activity of the turbulent fluxes which are treated differently by the ECMWF and TC scheme can indirectly be deduced from the surface fluxes of sensible and latent heat, because they are enhanced by larger upward transports aloft. On the global scale the θ-formula would produce similar q^2 fields, but a flux of sensible heat that is larger by 10 % and a latent heat flux smaller by 25 % during the first 24 hours. The impact on a particular situation like the cold air outbreak is, however, only marginal. The final thermodynamic profiles (mean over four model levels in the PBL) after 24 hours are only cooler by 0.1 degrees which is the order of magnitude of the changes between the TC scheme and the operational scheme. The choice of θ_v can, however, have a serious impact on the distribution of q^2 at a given model level by reflecting any noise existing in the moisture field.

b) Advection of TKE

Incorporating advective terms in the TKE equation requires far-reaching modifications to the model programming code. Therefore, the use of an additional fully prognostic variable has to be thoroughly justified. The extended scheme has only been developed after some confidence had been gained with the non-advective scheme. As a first applicatiion the cold air outbreak was chosen as it was believed that any sensitivity to the additional terms would become obvious in this case. The q^2 field has been monitored, so that whenever they occurred, negative values were set to zero.

Comparison of this integration with the previous ones, however, showed only a small impact on the performance of the scheme. The saturation layer between 950 and 850 mb has now a slightly warmer top (Fig. 10d) but is otherwise the same. On the global scale, a sensitivity of the distribution and level of TKE is more obvious. Fig. 11 and 12 show the instantaneous global TKE field after 24 hours into the integration in both cases. Larger areas are now turbulent, but the resulting turbulent fluxes of sensible and latent heat on the global scale are not substantially altered. Although the global effects don't seem to be very large, the high local sensitivity is one arguement to retain advective terms in the TKE equation.

c) Inexpensive formula for K

Kolmogorov's (1942) expression $K = c\ell q$ has been used in several applications (Rodi, 1980; Melgarejo, 1980) in order to take advantage of the additional information given by TKE, but also to reduce calculation costs. This approach was also tested as an alternate formulation. Although it provides turbulent kinetic energy in the planetary boundary layer that is very similar to the control scheme, it cannot represent TKE in the free atmosphere due to an initialisation problem. During the period of adjustment from the balanced initial q^2 field to the interactive one, values may become negative above the PBL, where the source terms in the equation are small. Diffusion of TKE from the lower levels is not strong enough to refill the reservoir aloft, so that negative values set to zero remain zero during the rest of the integration. Several vertical levels of zero TKE, however, subsequently reduce the length scale parameter, so that eventually less mixing occurs. Over the time scale of the air mass transformation this leads to unacceptable differences in the thermodynamic structure as compared to the control run.

d) The free atmosphere

It has been mentioned before that the TC scheme is based on boundary layer approximations and that accordingly turbulence is assumed to vanish at $R_{i,cr} = 0.21$.

When the operational ECMWF model was found to give a too high heat transport near the tropopause level this was attributed to the fact that it had no critical Richardson number cut-off (Louis et al., 1981). Subsequently, it was modified in order to achieve a cut-off at $R_{i,cr} = 1$ in the free atmosphere

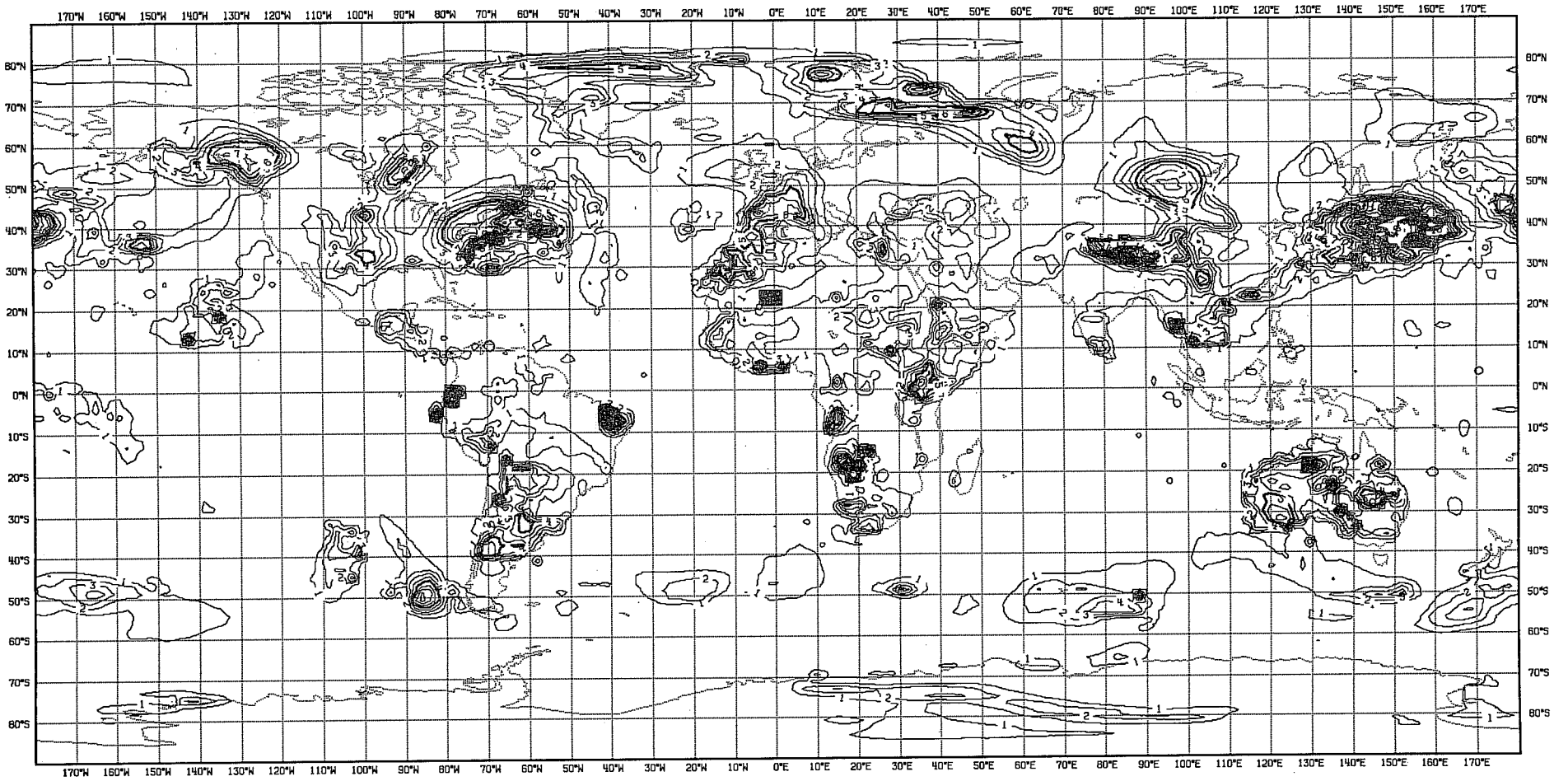

Fig. 11 Global distribution of turbulence kinetic energy q^2 averaged over model levels 13-15. TM without advection of q^2.

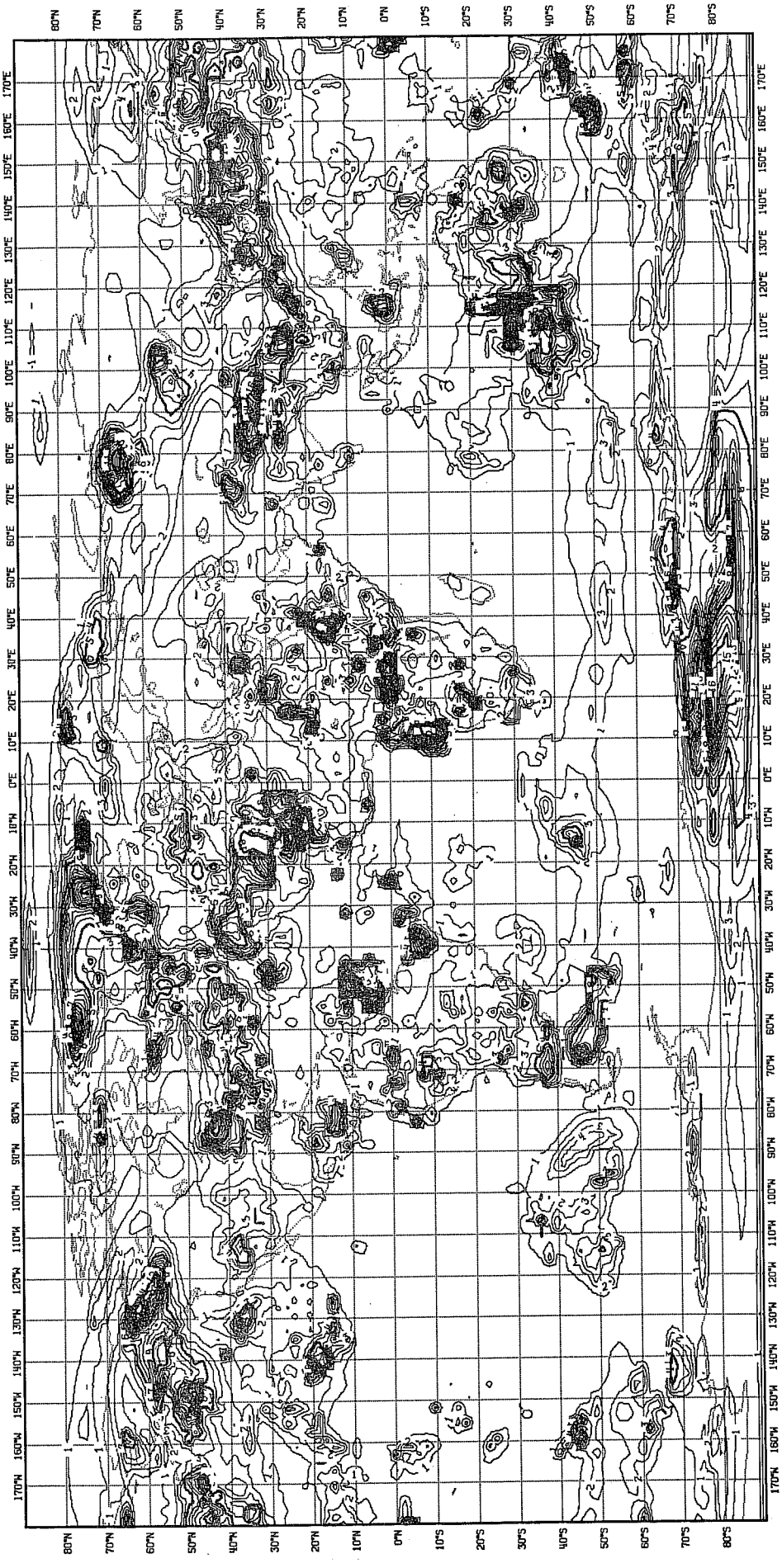

Fig. 12 As Fig. 11, but for TM with advection of q^2.

thus producing less heat transfer and at the same time allowing for a secondary maximum of dissipation of kinetic energy at upper levels. Examination of the global integral of dissipation over all levels reveals that only about half of the total is dissipated in the PBL and the rest is due to momentum transfer in the free atmosphere. With the TC scheme the total dissipation is reduced by 40%.

A detrimental effect due to the non-local prescription of the length-scale parameter ℓ has been ruled out by sensitivity tests. A set of prescribed asymptotic values of ℓ_o (150, 300, 450 m) independent of TKE in the PBL was used in 24 hour global test integrations. With increasing ℓ_o the global budget values of sensible and latent heat flux were increased, but the integral value of dissipation only changed by a small fraction. The scheme's applicability is basically restricted by the choice of empirical constants and as far as a global model is concerned the expense incurred by an additional prognostic equation for ℓ is not justified.

Preliminary 10 day integrations have shown a considerably strong positive impact on the flow due to the lack of dissipation in the upper model atmosphere. In one particular case a trough developed in the 500 mb height field off the East-coast of North America at day 6 which compared very favourably with the corresponding analysis. This trough did not develop in the control integration until one day later. The TC scheme with its slightly higher surface fluxes and a lack of dissipation at upper levels was able to balance errors in the initial fields which lead to an erroneous development in the control run, but in this particular case, the reduced dissipation had the strongest impact on the evolution on the flow.

The secondary maximum of dissipation that has been reported by Kung and Baker (1975) might not be entirely related to vertical mixing processes such as clear air turbulence (Trout and Panofsky, 1969) but to horizontal small-scale processes (Holopainen and Nurmi, 1980; Holopainen, 1982). Diagnostic studies have pointed to the fact that in mid-latitudes there is a large longitudinal variation of areas with positive and negative viscosity at upper levels, in general balancing the PBL dissipation (Kung, 1967, Kung and Baker, 1975, Holopainen and Eerola, 1979). A tuning towards a situation where there is systematically a positive dissipation may not always produce realistic conditions and may lead to an erroneous evolution of the flow. This is

particularly important as changes in the momentum transfer seem to have the most direct impact on the flow, whereas latent and sensible heat fluxes are only influential via the numerous feedback mechanisms. A considerable effect by mountains on the air current flowing over them has been established (Holopainen, 1982). Vertical momentum flux induced by mountain waves has e.g. been studied by Klemp and Lilly (1980). The parameterisation of these processes, however, cannot be achieved by the TC scheme and ought to be treated separately.

4.2.3 10 day forecasts

In the global forecasting model the application of the turbulence closure scheme is extended from the well-defined slightly stable or well-mixed situation to a wide range of thermodynamic structures. The vertical diffusion scheme is in this context not only responsible for the definition of the PBL thermodynamics and momentum transports but enters a feedback loop together with the convection, surface and radiation parameterisation. Energy transports by either scheme depend crucially on how the remaining parameterisations react to them. Increased vertical diffusion in the PBL may cause an increase in the moisture input for the convection scheme, but on the other hand convection schemes based on different methods may themselves enhance surface layer transports and boundary layer fluxes by creating different thermodynamic structures above the PBL.

Although it is therefore essential to study the performance of the vertical diffusion scheme at isolated points it is also important to monitor the overall effect on the flow, its energy budget and the representation of fields in a climatological sense.

Global 10 day forecasts were initialised from the FGGE analyses of 21 January 1979 12Z and 11 June 1979 12Z. Both the winter and summer case were integrated using the standard ECMWF gridpoint forecasting model (control) and the version where the vertical diffusion scheme was replaced by the TC scheme without advection of TKE. As special cases the winter integrations were repeated with advection of TKE included and also with diurnally varying radiaton input.

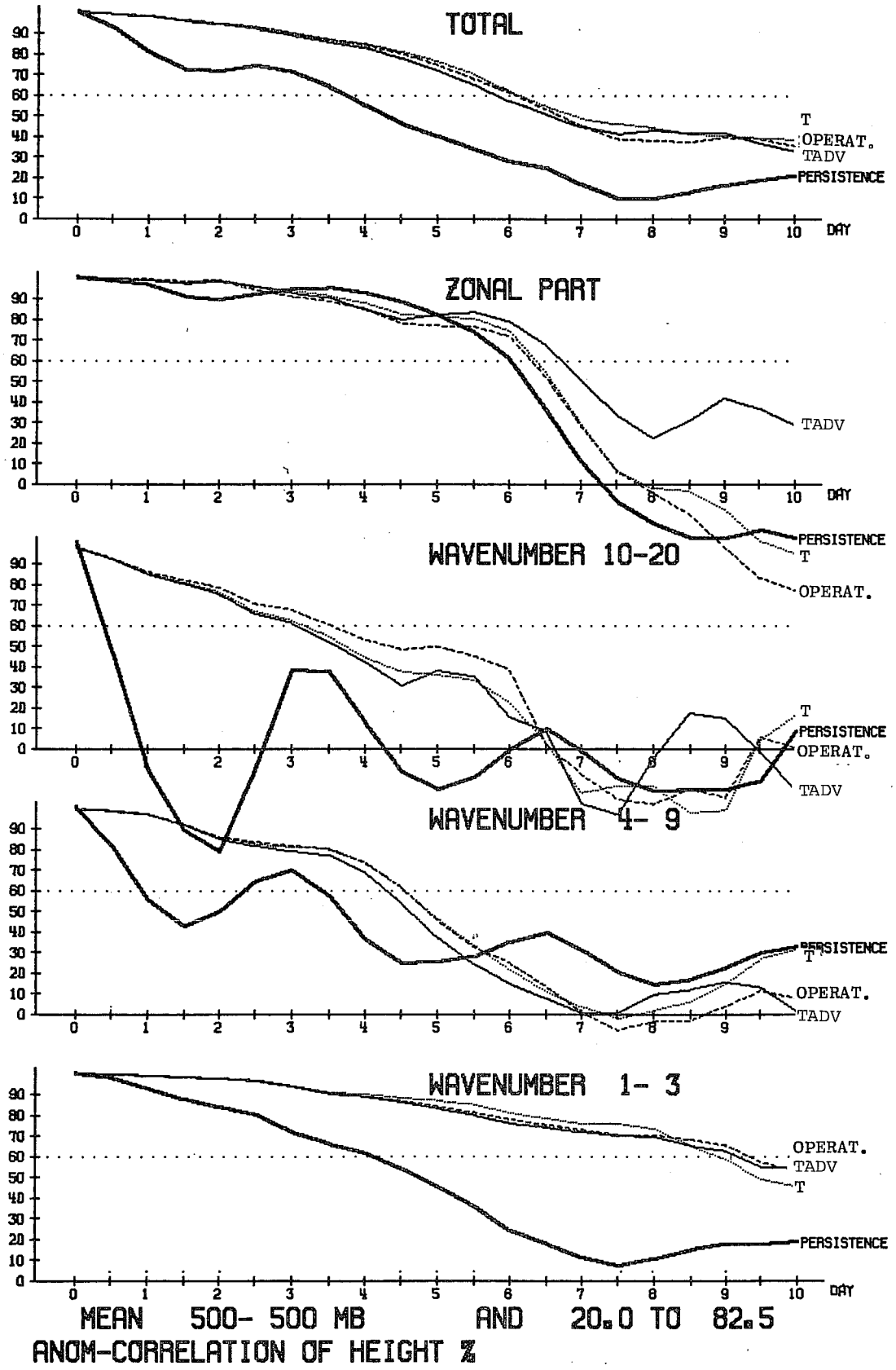

Fig. 13 Anomaly correlation of the 500 hPa height field for a winter 10 day integration (from FGGE analysis of 21/1/1979 12Z). The 60% level indicates the limit of usefulness of the forecast. Operational scheme (OPERAT), turbulence closure scheme without (T) and with advection of q^2 (TADV).

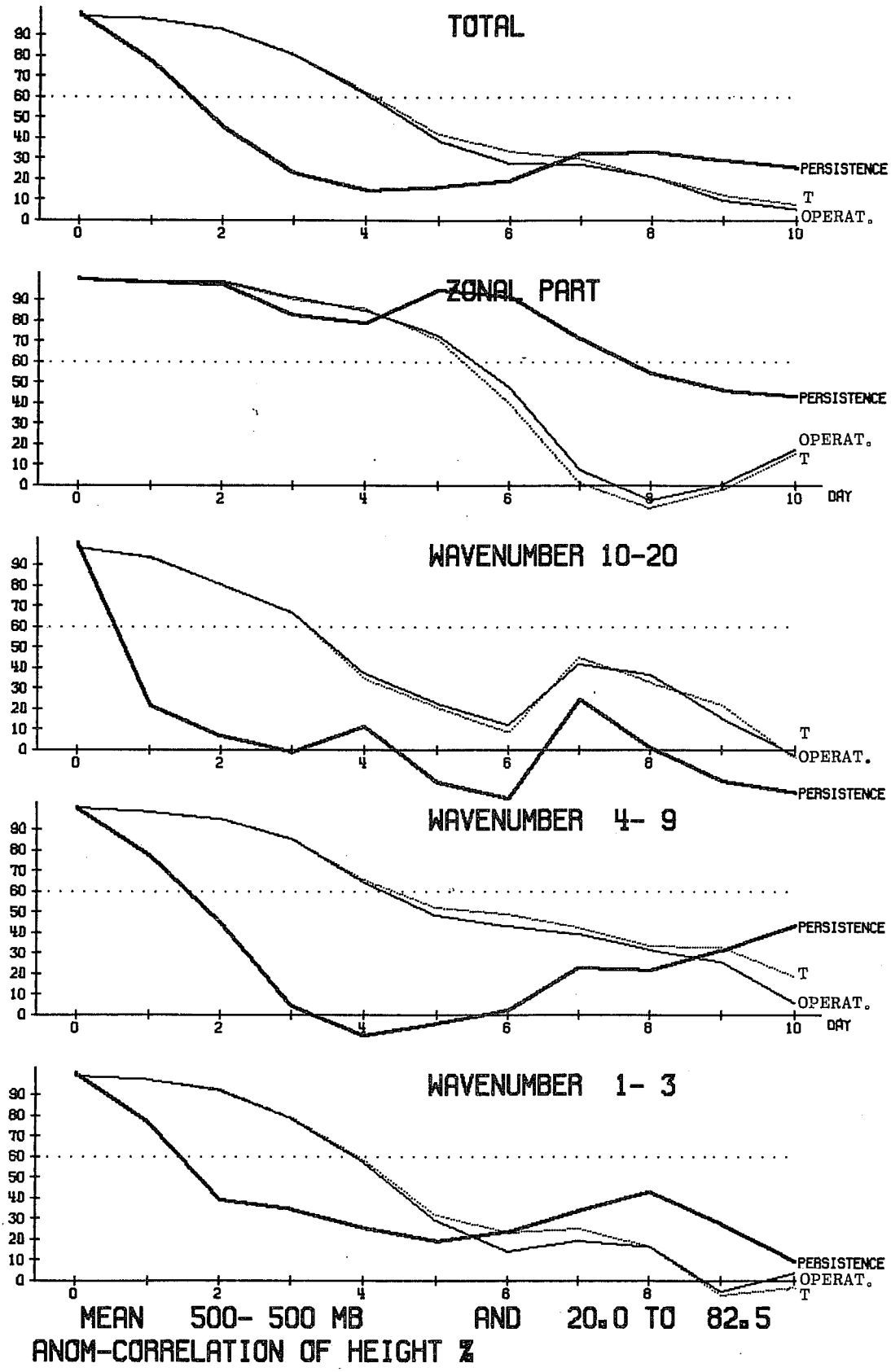

Fig. 14 As for Fig. 13 but for the summer case of 11/6/1979 12Z.

Any sensitivity to changes in the parameterisation package is reflected in the performance of the model. Anomaly correlations of height at 1000 or 500 mbar show a small positive impact of the TC scheme at mid-latitudes (Fig. 13 for the winter, Fig. 14 for the summer case). The evolution of the flow with either model configuration is equal to up to day six in the winter and four in the summer case (Fig. 15). After that the TC scheme manifests a positive impact, largest beyond the 60 % threshold of usefulness of the forecast. Concentrating on the winter case, Figs. 16a and b compare the tendencies DT for temperature and DS for moisture due to turbulent diffusion for the ECMWF and TC scheme, respectively. The top of the boundary layer is remarkably well-defined in both cases, but slightly lower in the TC case. The main difference between the two schemes is the downward flux above the PBL top in the TC scheme. Otherwise the results agree in many details.

Globally, and with both schemes, the centers of fluxes of sensible and latent heat (Figs. 17 and 18a and b) are distributed over the globe according to the same realistic pattern (Tiedtke, 1981). In TC the sensible heat flux is in general slightly reduced in some unstable situations and the downward fluxes are enhanced in stable situations, the latter being the more pronounced effect as it modifies the whole thermodynamic structure in some mid-latitude areas in the course of the 10 day integration. Therefore, differences between the fluxes in the two schemes are only pronounced in the mid-latitudes of the winter hemisphere. It is difficult to judge whether these are of the right order of magnitude as no independent source of data in elevated regions exists. Otherwise comparison with climatology (Budyko, 1974) shows good agreement of the geographical distribution of sensible heat fluxes in winter. Over the continents the moisture flux does not change much with TC, but over the northern parts of the oceans there are substantial increases of both sensible and latent heat fluxes (see also Figs. 21 and 22). The effect of the inclusion of advective terms into the q^2 equation further increases the latent heat flux. This increase seems to be larger than the model requires, because the slight improvement in the scores achieved by the TC scheme is turned into a worsening by the same small amount.

More pronounced moisture transports lead to an increase in convective activity, not necessarily creating new areas of activity, but enlarging the overall amount of precipitation during the 10 day period (Figs. 19a and b).

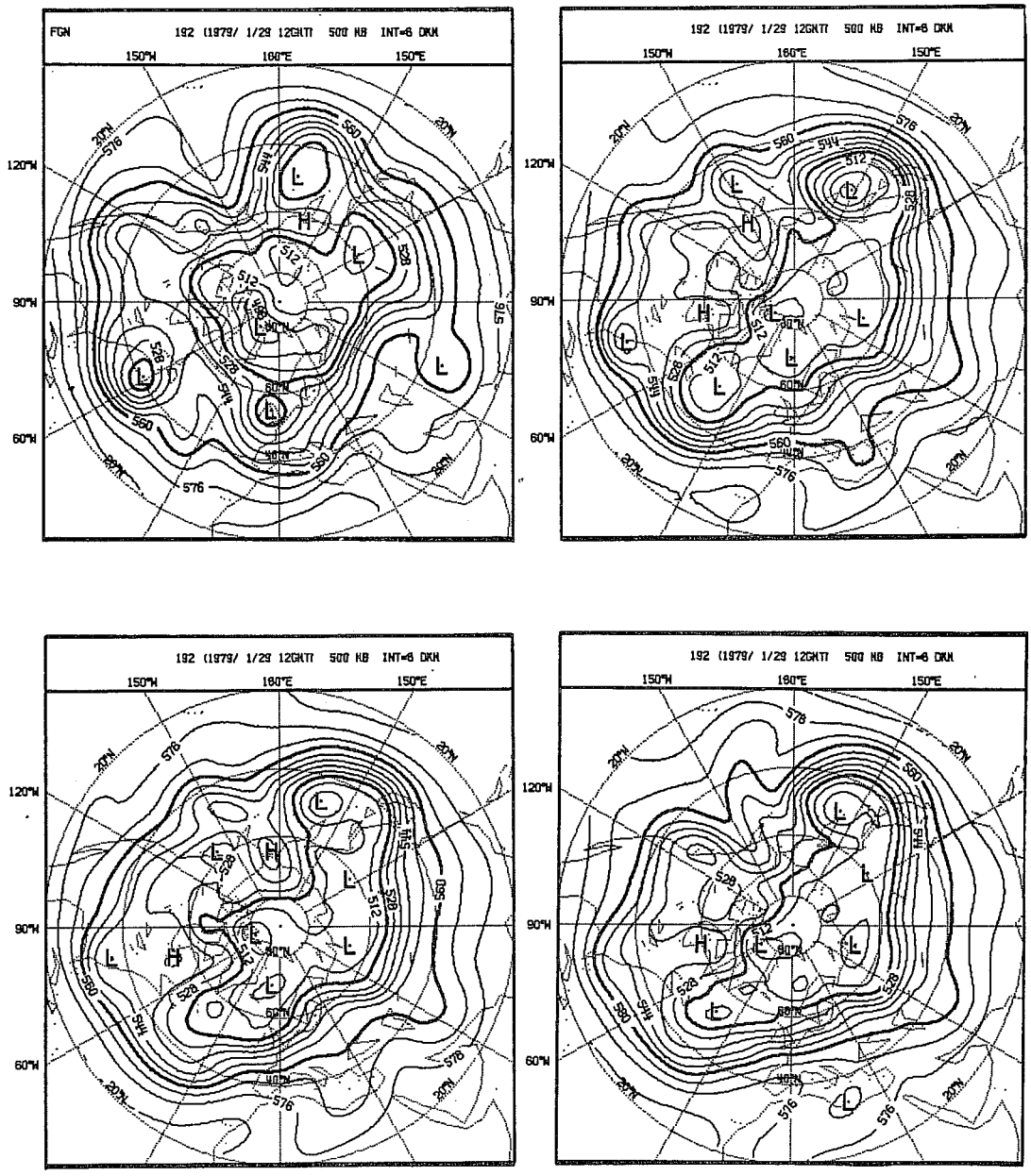

Fig. 15 Northern hemisphere maps of the 500 hPa height field at day 8 of the integration. FGGE analysis (top left), operational scheme (top right), turbulence closure scheme without (bottom left) and with advection of q^2 (bottom right).

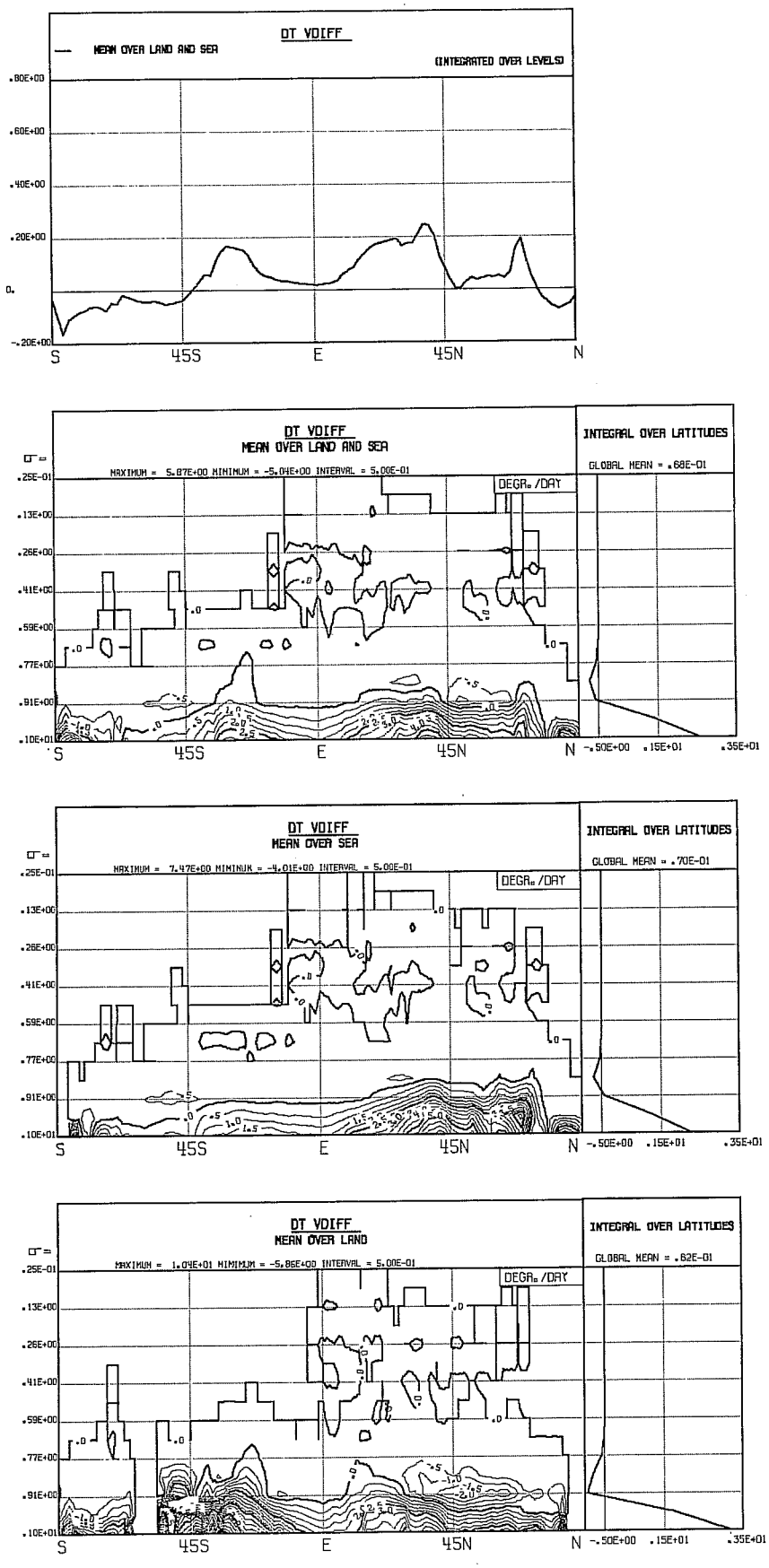

Fig. 16a Zonal mean values of net heating DT due to vertical diffusion for the turbulence closure scheme.

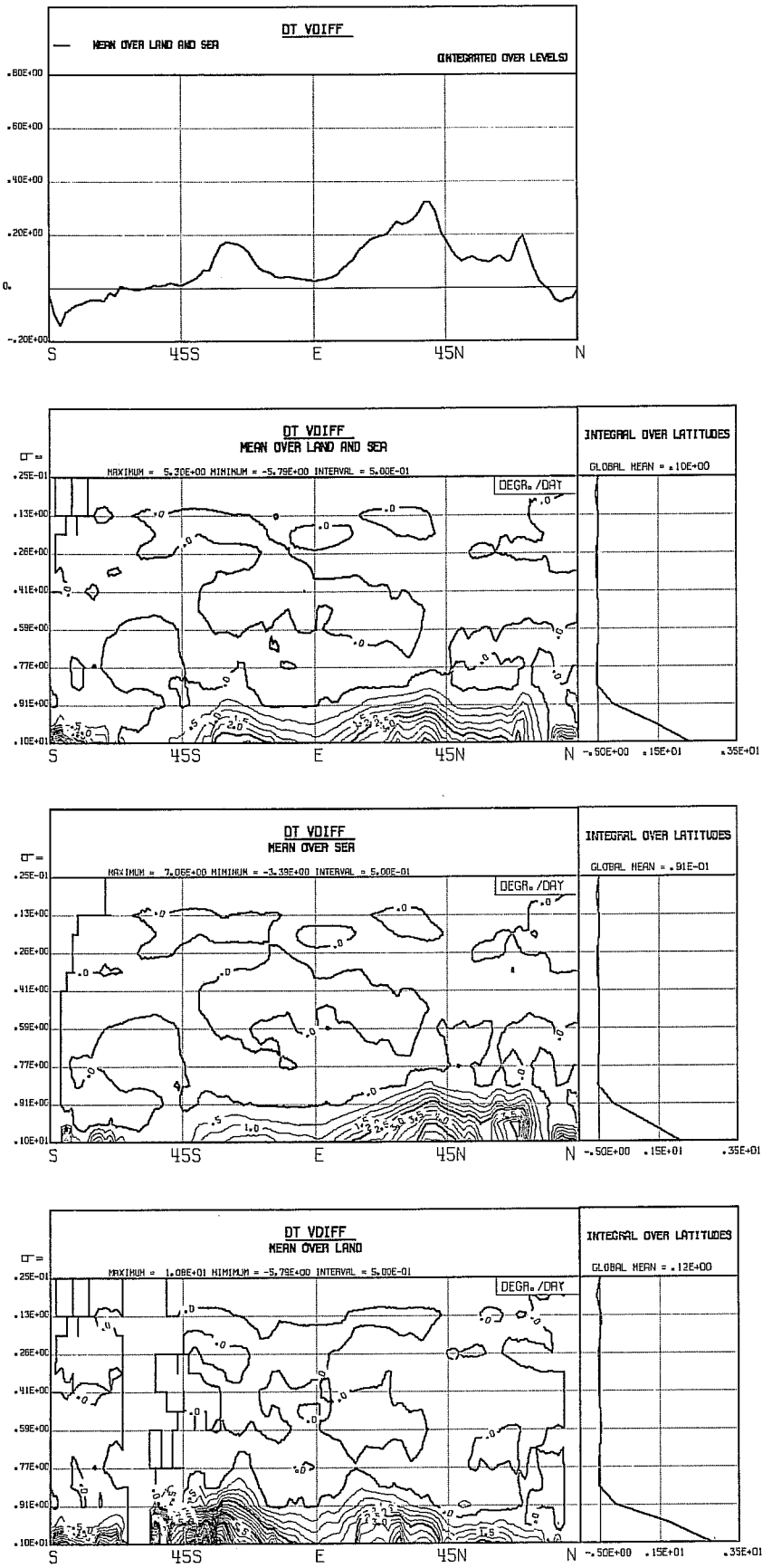

Fig. 16b As Fig. 16a but for the operational scheme.

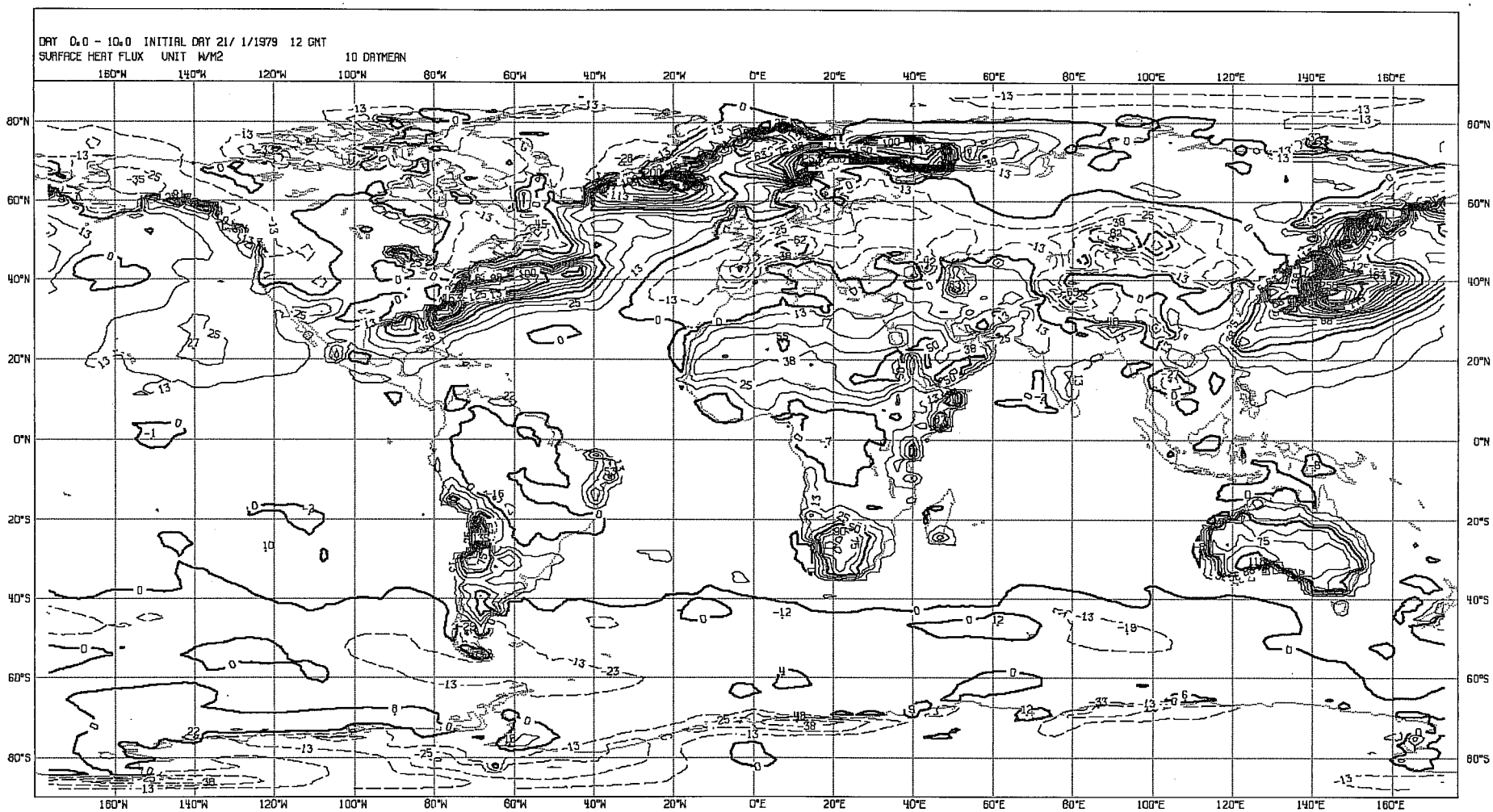

Fig. 17a Global distribution of sensible heat flux at the surface for the winter integration: turbulence closure scheme (TM).

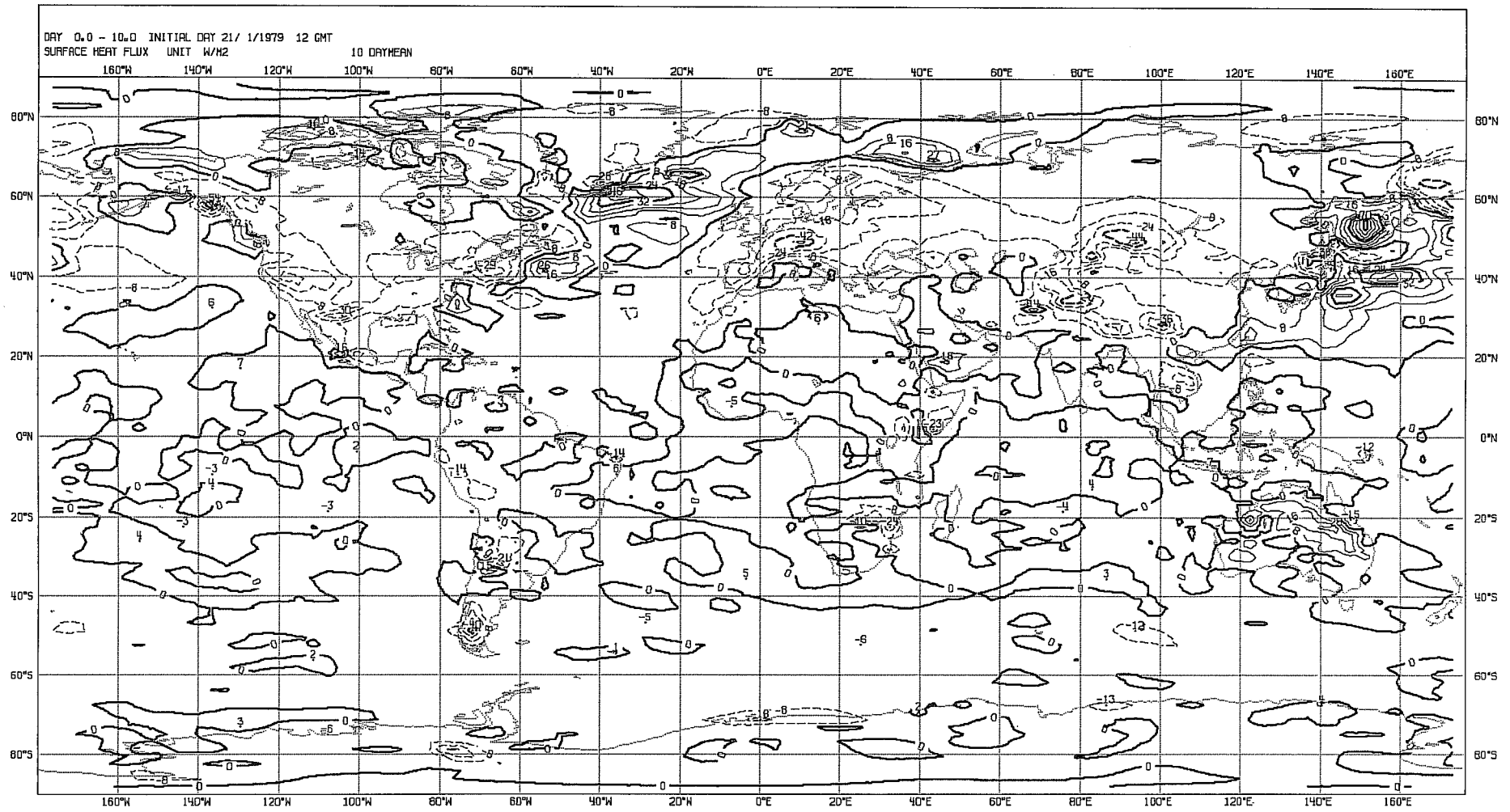

Fig. 17b As Fig. 17a but for differences between TM and the operational scheme.

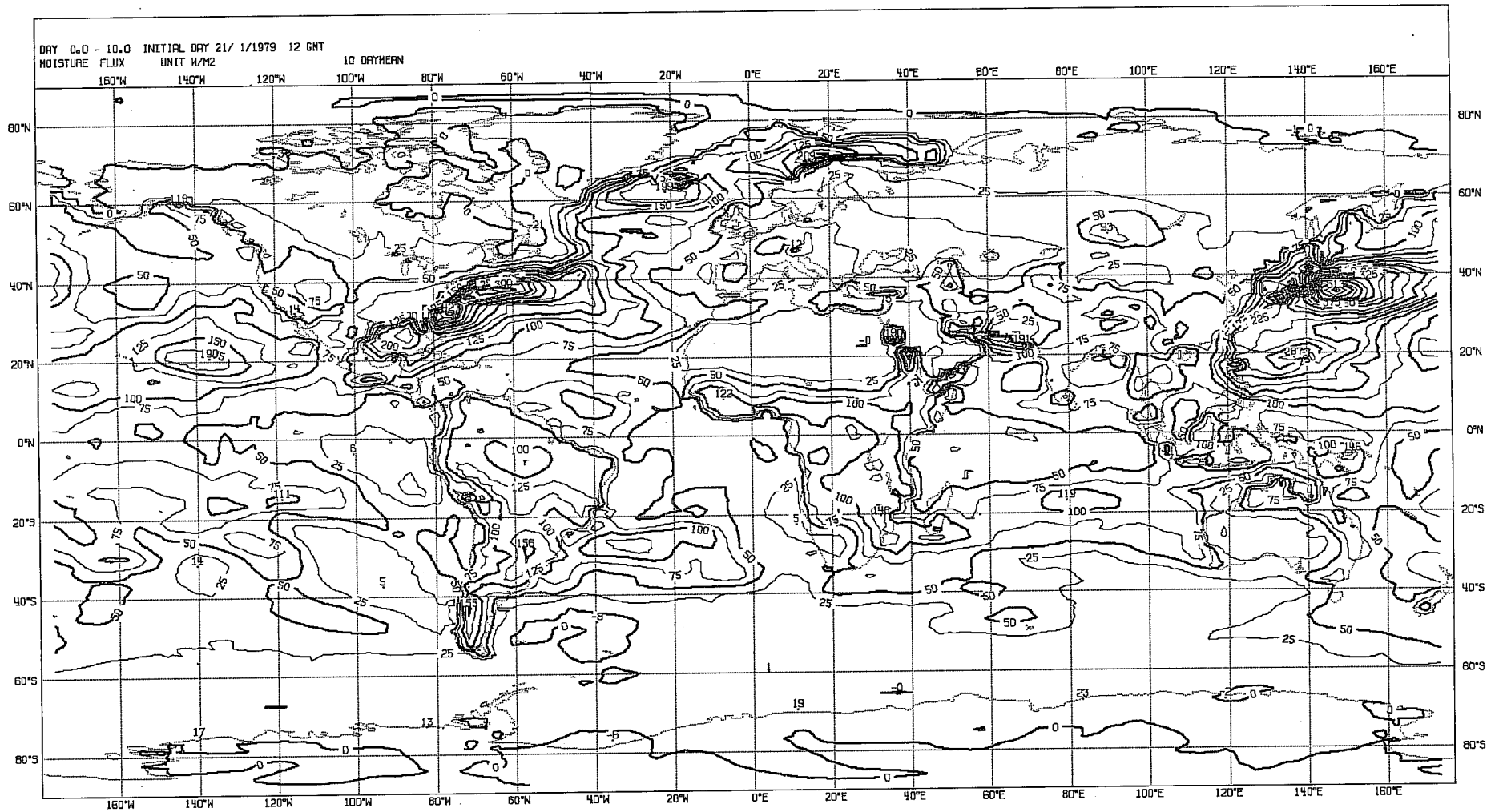

Fig. 18a Global distribution of latent heat flux at the surface for the winter integration: turbulence closure scheme (TM).

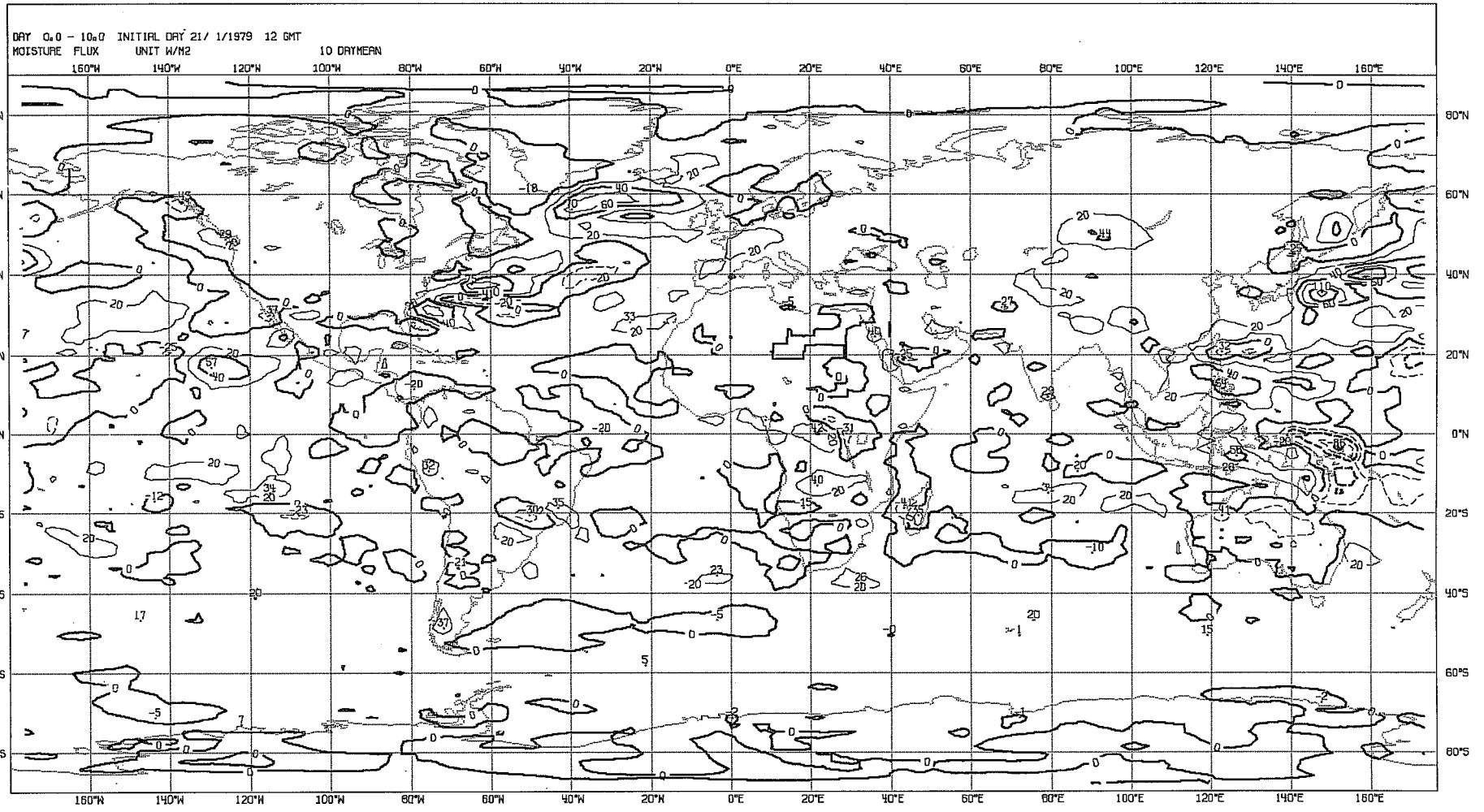

Fig. 18b As Fig. 18a but for differences between TM and the operational scheme.

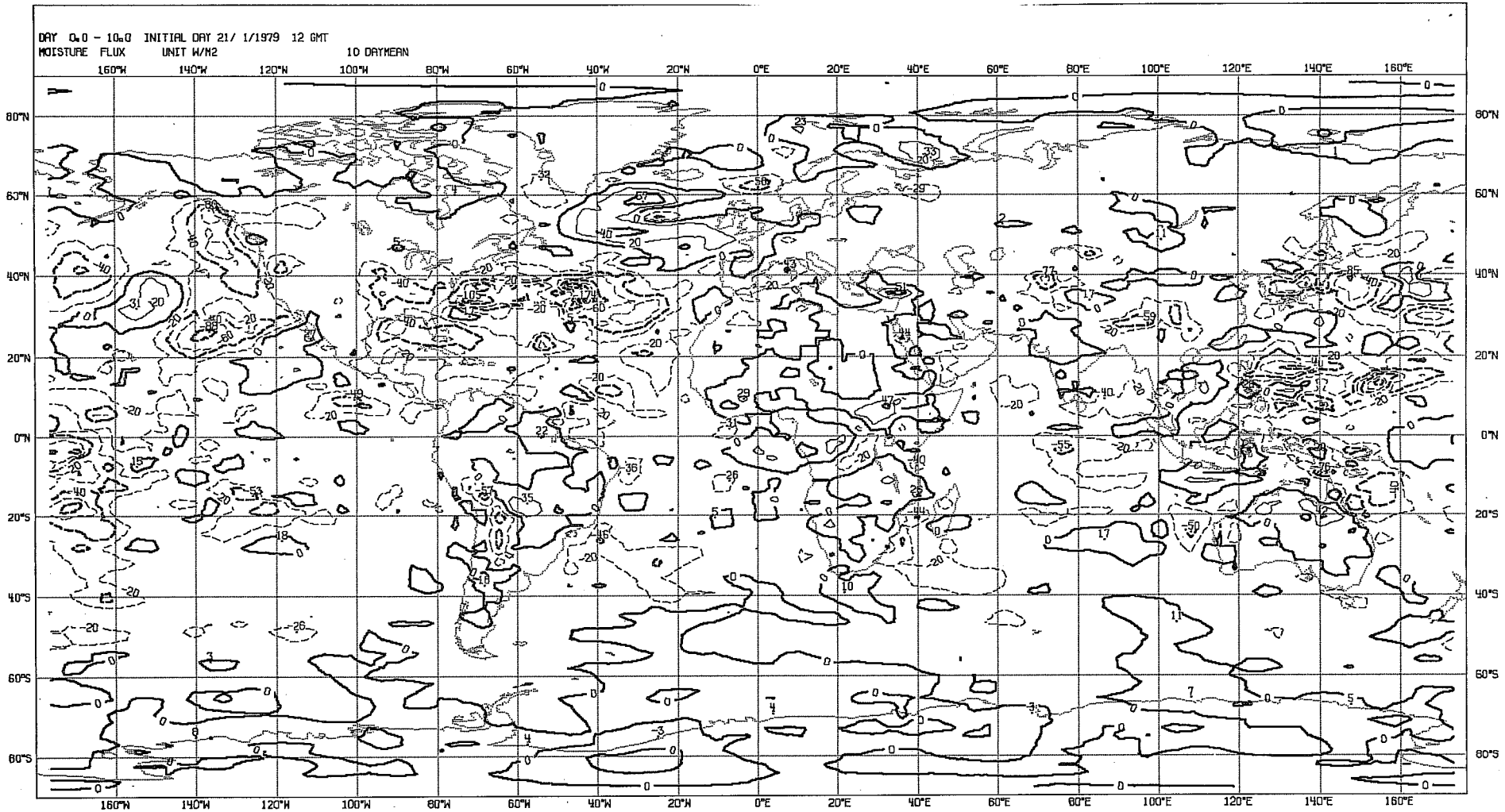

Fig. 18c As Fig. 18a but for differences between TM without and TADV with advection of q^2.

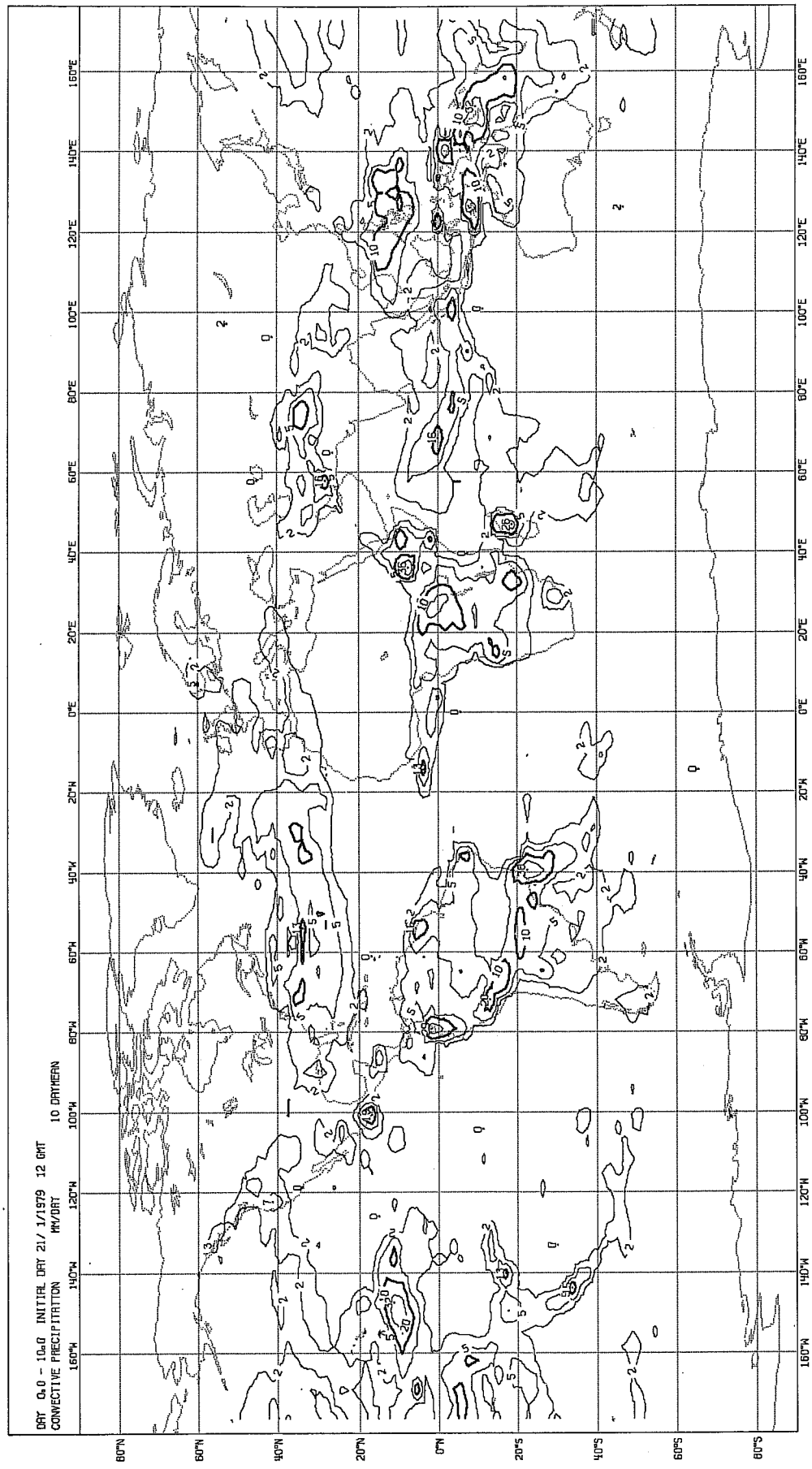

Fig. 19a Convective precipitation for the winter integration: turbulence closure scheme TM.

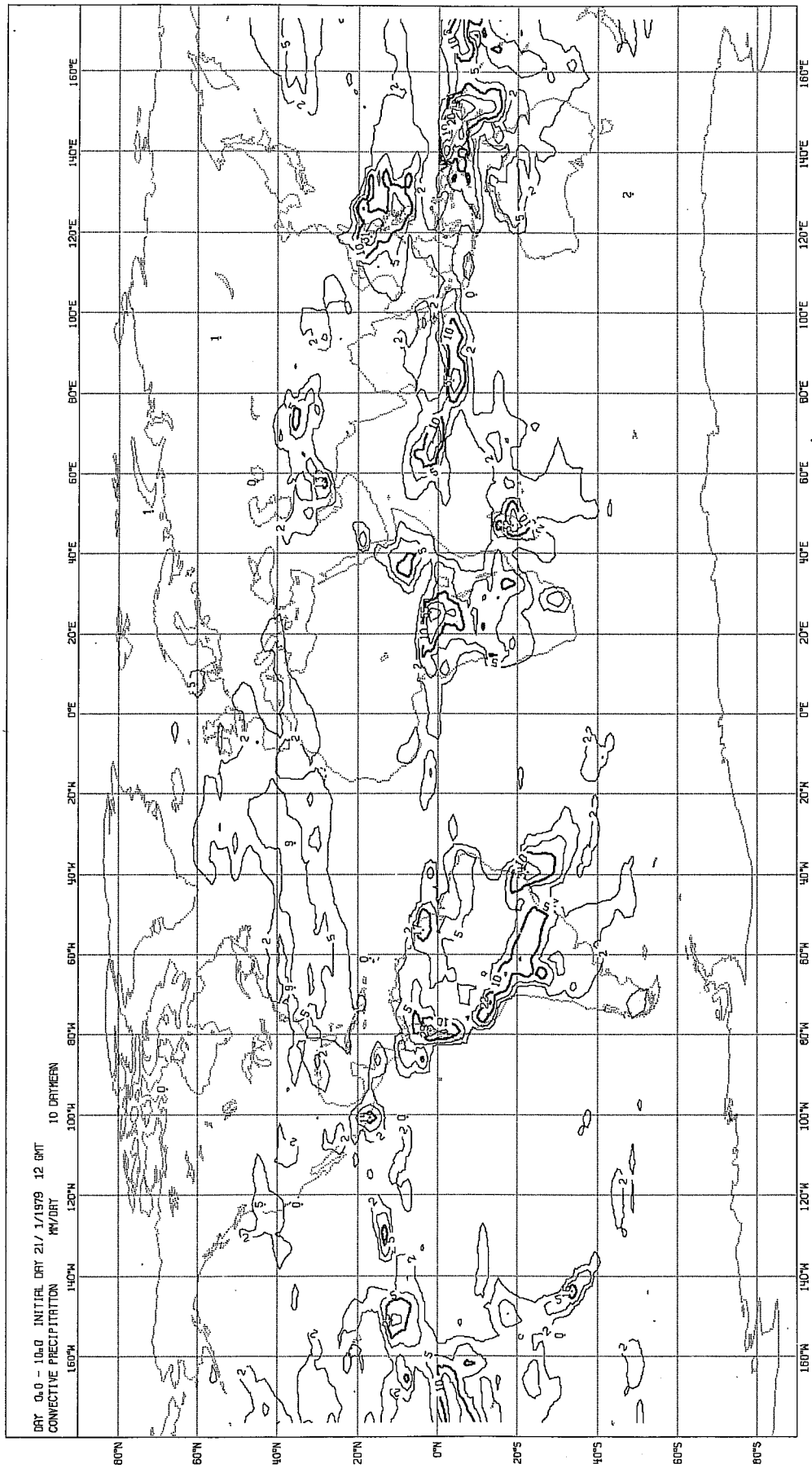

Fig. 19b As Fig. 19a but for the operational scheme.

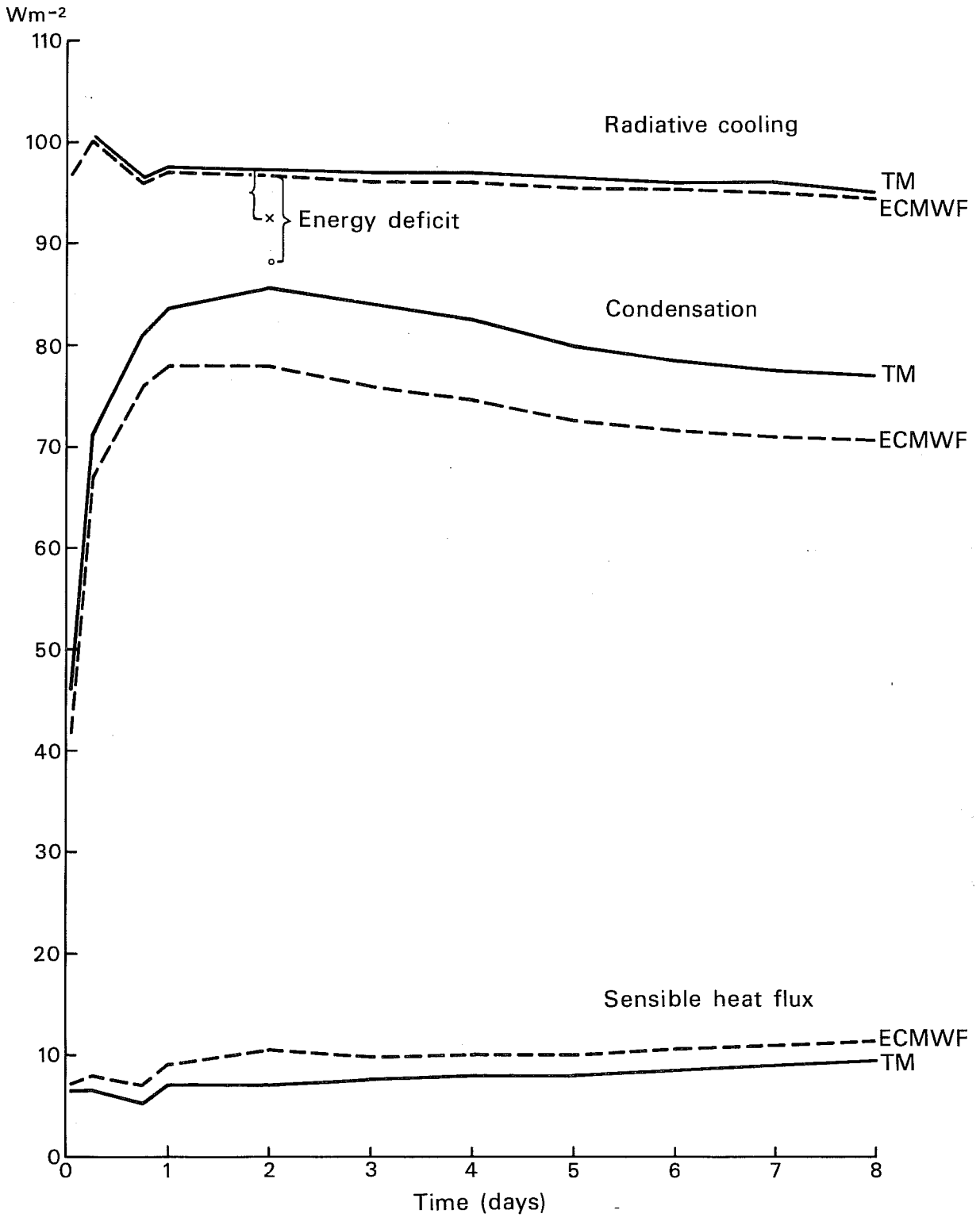

Fig. 20 Energy budget of the model integration for the winter case. The energy deficit is calculated as the difference between radiative cooling and the sum of heating due to condensation and sensible heat flux.

The same is true in the simulation of the summer forecast. The main advantage of the enhanced transport is its capability of reducing the energy deficit (Fig. 20) in the model integration which would lead to a cooling during the later stages of the forecast. This systematic error is even better reduced if the TC scheme is combined with the diurnal variation of radiation input (diurnal cycle) in the model. But, unfortunately this does not improve the performance of the model beyond that of the TC integration shown in Fig. 13 (no diurnal cycle).

4.2.4 50 day integrations

Integration of the model incorporating the TC scheme has also been extended up to 50 days. Here, the TC scheme proved to be a stable diffusion scheme providing a good geographical distribution of fluxes of sensible and latent heat. Due to the lack of independent data, verification of the 30-day mean values is restricted to monthly climatic values. Fig. 21 and 22 show monthly climatic values over the oceans compiled by Esbensen and Kushnir (1981). Maxima along the North-Eastern coasts of the continents are positioned as well as in the operational model (Tiedtke, 1981), but with higher values. Good agreement is also found along the zone of downward fluxes in the southern hemisphere, the maximum of which is better placed (by the southern tip of Africa) than in the operational case. The global distribution of cloudiness and precipitaion averaged over the 30-day period is again similar in both schemes. The TC scheme extends the western boundary of the ITCZ over Africa along the Ivory coast further than the operational one, but still lacks this feature over the Atlantic.

Even though the model has the desired larger energy input via the PBL, energy conversions and large-scale transports still show various deficiencies that have become known to be systematic model features. While there is a persistently positive impact on the forecast in mid-latitudes, diagnostics of the model performance in the tropics display that its generally poor forecasting skill is not improved by the TC scheme and the resulting enhancement of convection. Convection is slightly stronger over most ocean areas and heavily reduced at single spots with too intense activity in the control run because of a reduction in the turbulent fluxes in these places. The TC scheme has an increased surface stress in mountaineous regions in the

winter-hemisphere mid-latitudes and very stably stratified areas (Fig. 23). Differences can amount to up to 50 % of the value in the control run. As the stress in the PBL is a parameter to which the flow is highly sensitive, consequently, there is a reduction of the baroclinic waves by Ekman pumping. Another effect that also acts in the same direction is convective heating in the cold air behind the surface troughs during their growth stage (Hoskins, 1980). These mechanisms further support the systematic error of the model rather than decrease it.

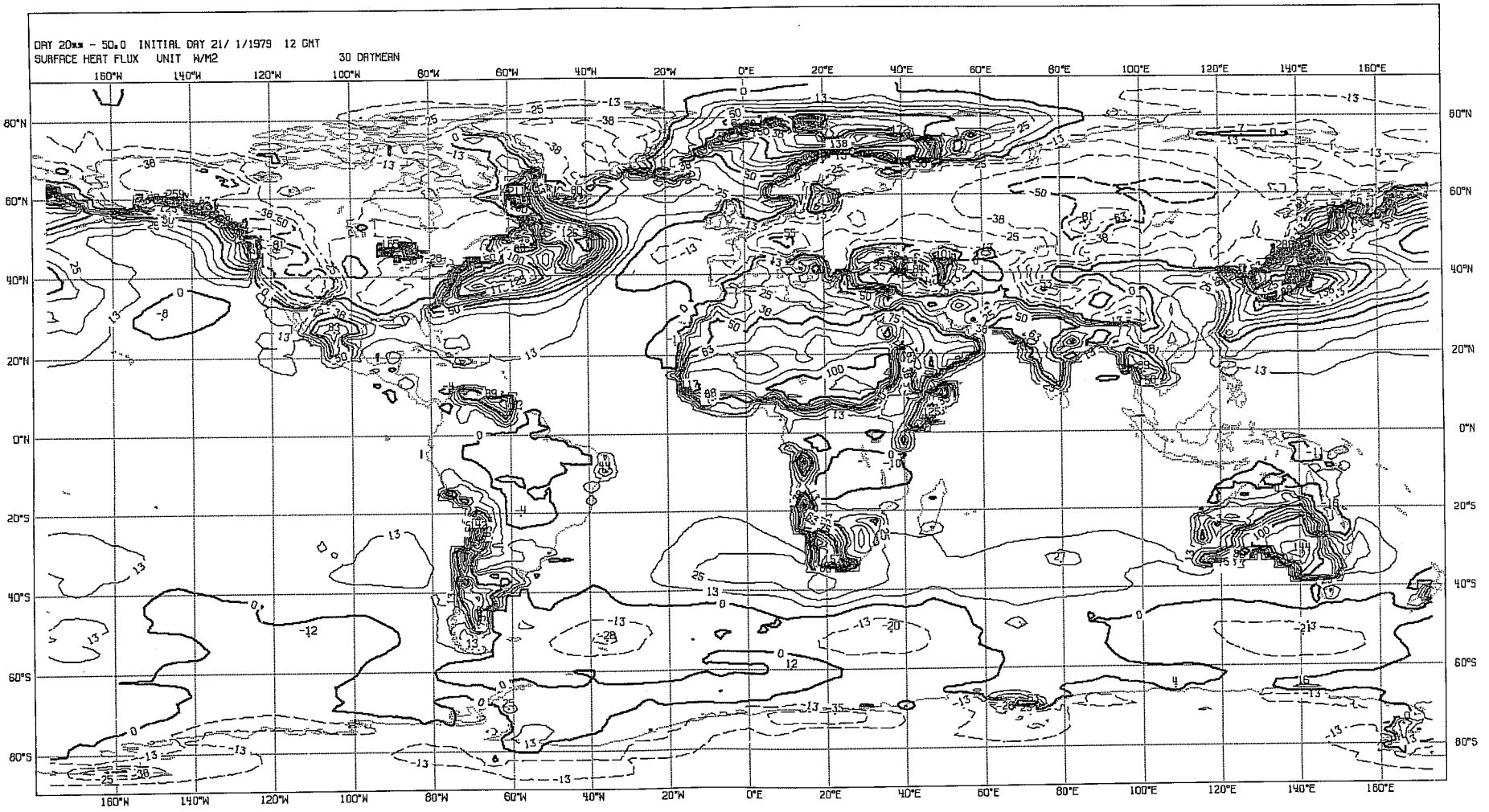

Fig. 21a Sensible heat flux at the surface averaged over the last 30 days of a 50 day integration: TM.

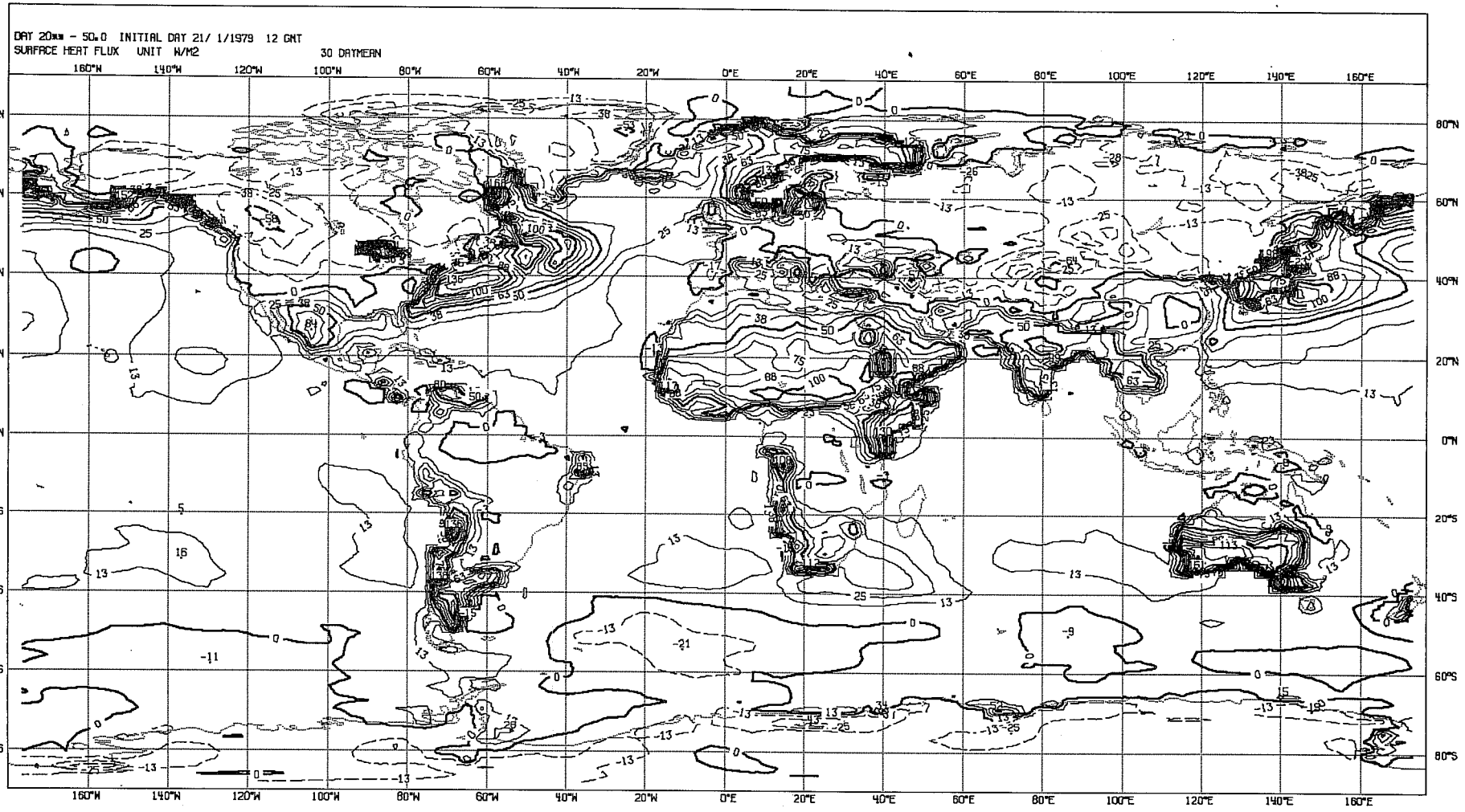

Fig. 21b As Fig. 21a but for the operational scheme.

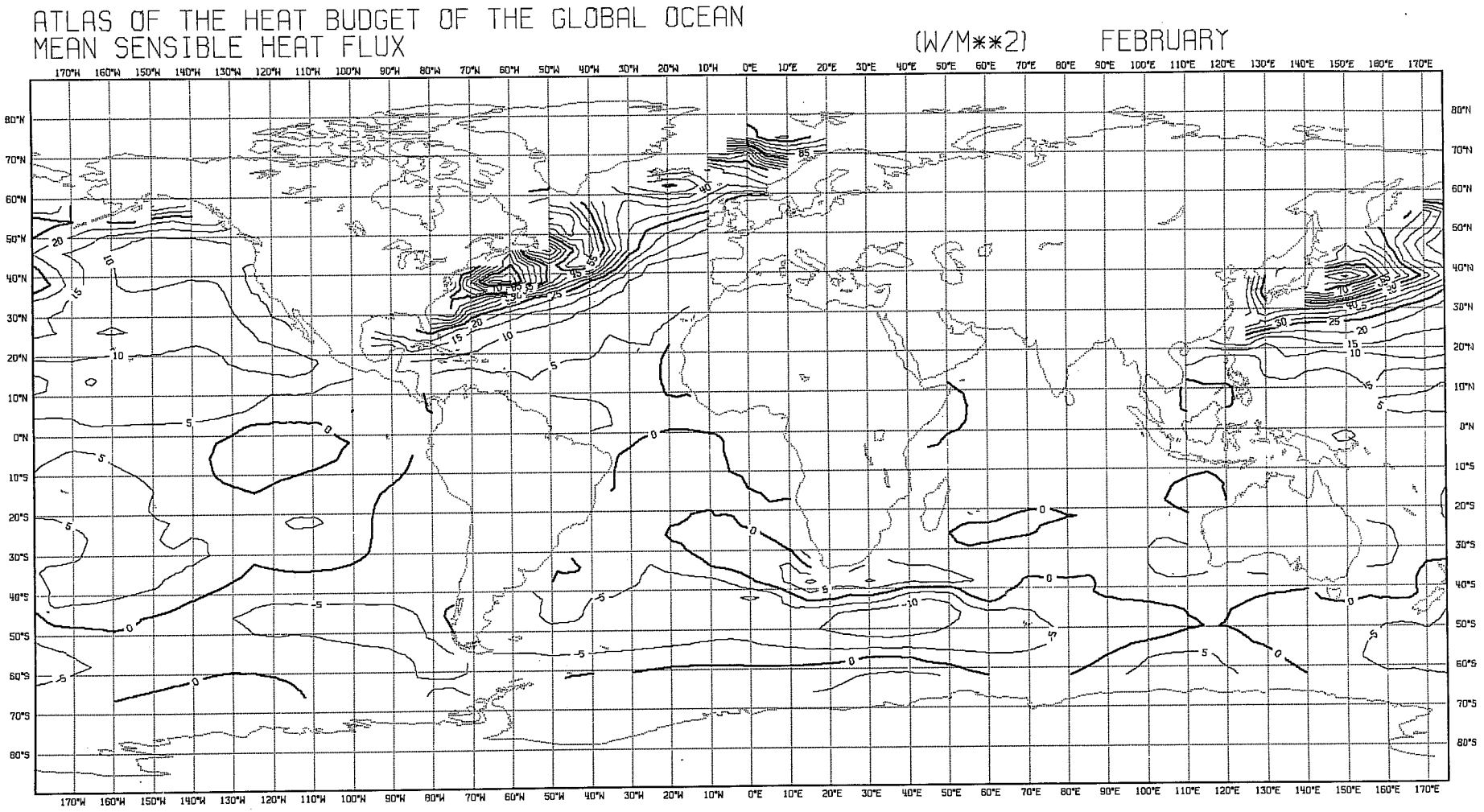

Fig. 22 Sensible heat flux climatology over the oceans by Esbensen and Kushnir (1981).

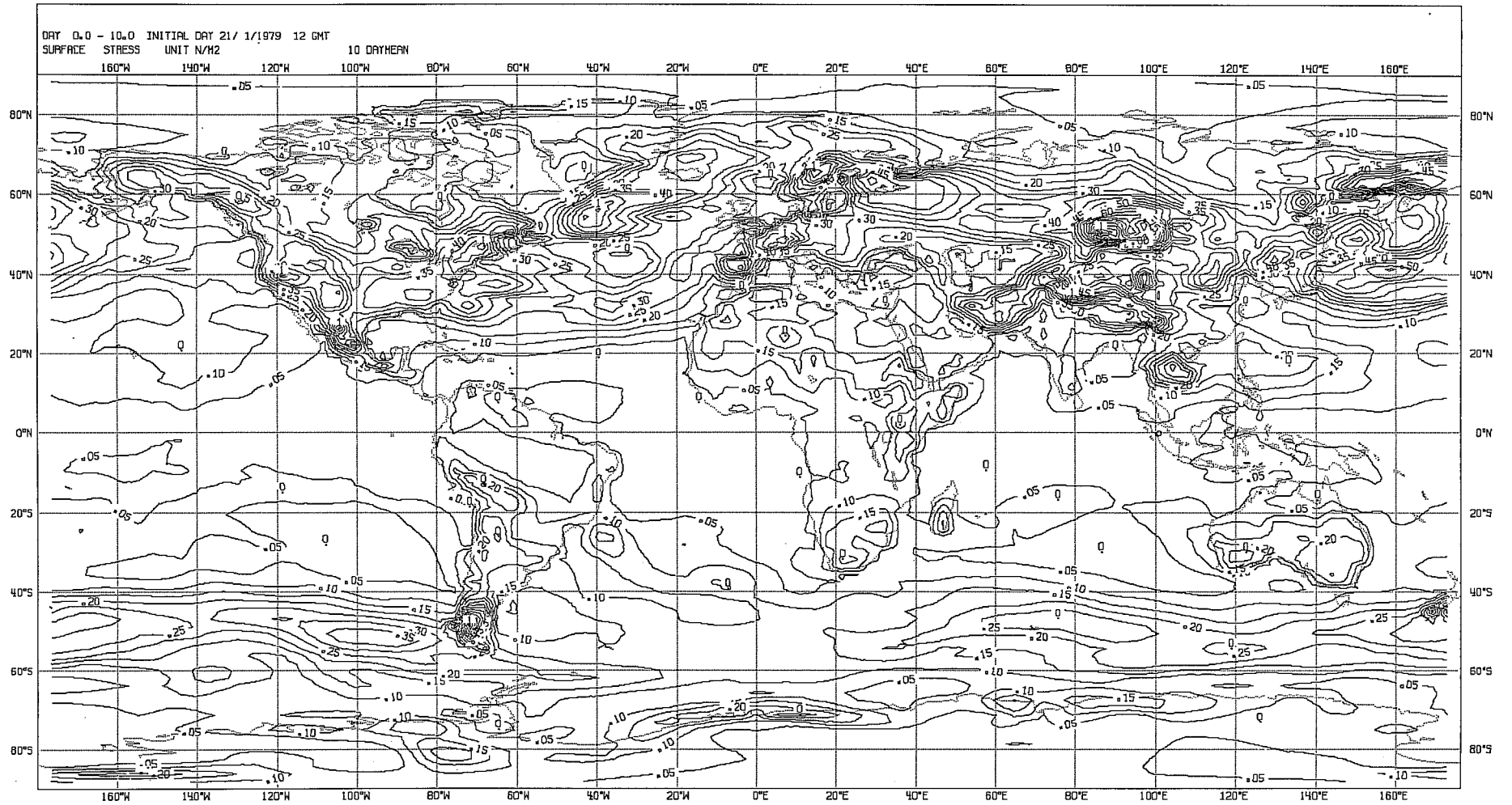

Fig. 23a Surface stress for the winter integration: turbulence closure scheme. TM.

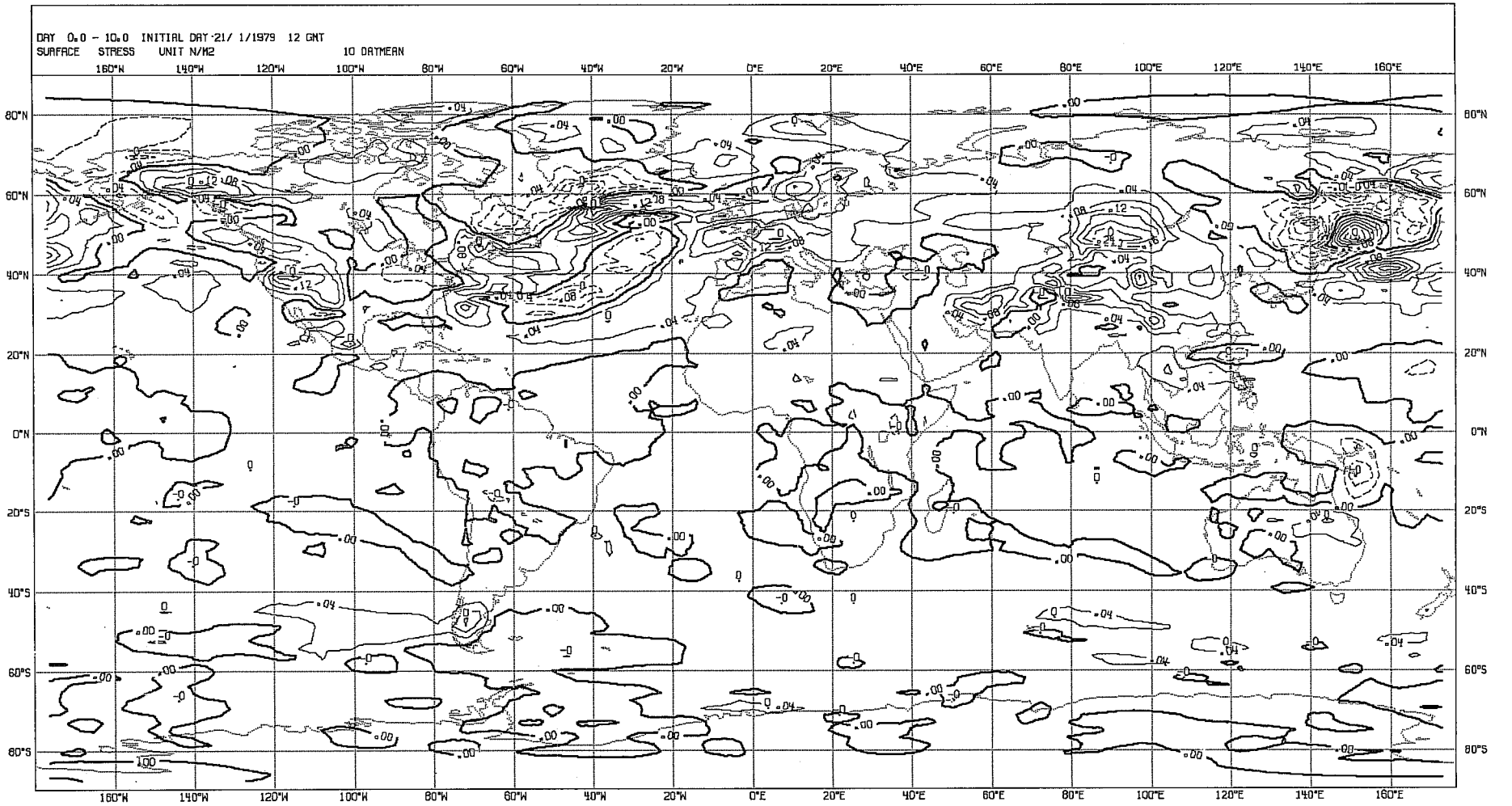

Fig. 23b As Fig. 23a but for the difference between TM and the operational scheme.

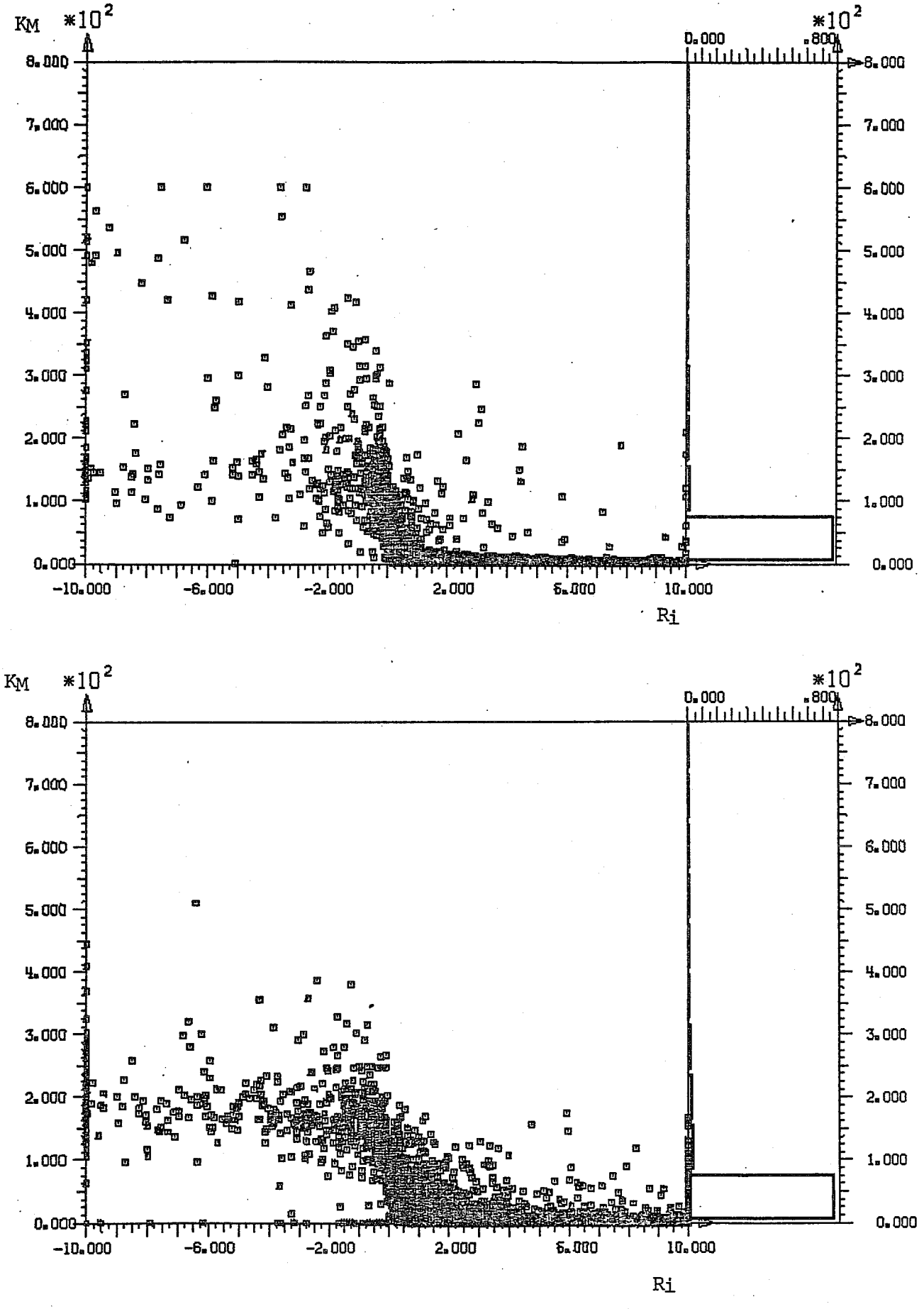

Fig. 24 Diffusion coefficient K_M versus Richardson number at model level 13.

5. CONCLUSIONS

The simplified second order closure scheme (Mellor and Yamada, 1974) that was adapted to fulfil the role of a parameterisation scheme for vertical diffusion in the ECMWF gridpoint forecasting model requires a large amount of computational resources because an additional prognostic variable for turbulence kinetic energy is integrated. Both the already quite elaborate operational stability-dependent first order closure ECMWF diffusion scheme and the turbulence closure scheme without advection of turbulence kinetic energy ("1.5 order closure") produce very similar diffusion coefficients. Fig. 24 shows a scatter-diagram of K_M versus Richardson number at a model layer in the PBL taken from all gridpoints at a certain timestep of a global integration. K_M appears to be confined to a smaller range and is more accurately defined by the TC scheme than by the operational one. This points to the fact that q^2 in the model without advective processes is always close to its equilibrium value.

The TC scheme represents an independent way to test the reliability and performance of the operational scheme that has been carefully developed, tuned and adapted to the model's needs. It has been shown that the more empirical ECMWF scheme reaches an approximately equivalent level of performance in the representation of PBL processes.

The change to a TC closure only has a marginal impact on the forecast in mid-latitudes, although it alleviates one particular aspect of the model's systematic deficencies, the energy deficit. Even though the scheme may be more accurate and physical in high resolution environments, most benefit is lost through truncation errors in the large scale model. Due to the sensitivity showed with regard to advection of TKE, it is advisable to always include these terms. This ought to be possible because they are only responsible for a small further increase in computational costs as compared to the basic scheme.

Originally designed to describe PBL processes, the scheme cannot provide dissipation of kinetic energy in the free atmosphere, which the operational scheme has been tuned to do. A separate parameterisation technique ought to be applied to this problem.

The turbulence closure scheme in the form presented here is only truely applicable in the dry case without phase changes. There is, however, potential to incorporate phase transitions by extending the set of equations. Further development of the scheme will have to go in this direction so that eventually a complete description of processes in the PBL including clouds can be given. Only if this can be achieved, a more sophisticated treatment of vertical fluxes of sensible and latent heat in the forecasting model will be justified. Due to the above limitations, the scheme is currently not considered for operational use.

The above conclusions are valid for the state of the model as it was when this study was undertaken. They should be reassessed in the framework of the spectral model and also in conjunction with the physics scheme incorporated in 1985.

References

André, J.C., G. DeMoor, P. Lacarrère and R. du Vachat, 1976: Turbulence approximation for inhomogeneous flows. Part I: The clipping approximation. J.Atm.Sci., 33, 476-481. Part II: The numerical simulation of a penetrative convection experiment. J.Atm.Sci., 33, 482-491.

Blackadar, A.K., 1962: The vertical distribution of wind and turbulent exchange in a neutral atmosphere. J.Geophys.Res., 67, 3095-3102.

Budyko, M.I., and D.H. Miller, 1974: Climate and life. Ac.Press, London, 508 pp.

Carson, D.F., 1977: Characteristics of the near-neutral boundary layer derived from the Leipzig wind profile data. Met. O 20, Technical Note No. II/104, Meteorological Office, Bracknell, U.K.

Carson, D.J. and F.B. Smith, 1971: A comparison of the conflicting wind-stress relationships formulated by Lettau and Swinbank on the basis of the Leipzig wind profile. Met.O 14 Turbulence and Diffusion Notes 17. Meteorological Office, Bracknell, U.K.

Carson, D.J. and F.B. Smith, 1973: The Leipzig wind profile and the boundary layer wind-stress relationships. Quart.J.Roy.Met.Soc., 99, 171-177.

Clarke. R.H., A.J. Dyer, R.R. Brook, D.G. Reid and A.J. Troup, 1971: The Wangara experiment: Boundary layer data. Techn. Paper 19, Div. Met. Phys. CSIRO, Aspendale, Australia.

Deardorff, J.W., 1972: Numerical investigation of neutral and unstable planetary boundary layers. J.Atm.Sci., 29, 91-115.

Deardorff, J.W., 1973: Three-dimensional numerical modeling of the planetary boundary layer. Workshop on Micrometeorology, Am.Meteor.Soc.,271-311.

Deardorff, J.W., 1974: Three-dimensional numerical study of the height and mean structure of a heated planetary boundary layer. Bound.Lay. Meteor., 7, 87-106.

Deardorff, J.W., 1974: Three-dimensional numerical study of turbulence in an entraining mixed layer. Bound.Lay.Meteor., 7, 199-226.

Donaldson, C. du P., 1973: Construction of a dynamic model of the production of atmospheric turbulence and the dispersal of atmospheric pollutants. Workshop on Micrometeorology, Am.Meteor.Soc.,313-392.

Etling, D. and H.W. Detering, 1983: Parametrisierung turbulenter Flüße in numerischen Modellen zur Überstromung von Topographien. Annalen der Meteorologie, 20, Selbstverlag des Deutschen Wetterdienstes.

Helfand, H.M. and J.C. Labraga, 1983: A level 2.4 second order closure model for the prediction of turbulence. Research Activities in Atmospheric and Oceanic Modelling, I.D. Rutherford (ed). Report No. 5, WCRP Numerical Experimental Programme.

Holopainen, E., 1982: Long-term budget of zonal momentum in the free atmosphere over Europe in winter. Quart.J.Roy.Met.Soc., 108, 95-102.

Holopainen, E.O. and K. Eerola, 1979: A diagnostic study of the long-term balance of kinetic energy of atmospheric large-scale motion over the British Isles. Quart.J.Roy.Met.Soc.,105, 849-858.

Holopainen, E. and P. Nurmi, 1980: A diagnostic scale-interaction study employing a horizontal filtering technique. Tellus, 32, 124-130.

Hoskins, B.J., 1980: Effect of diabatic processes on transient mid-latitude waves. Workshop on Diagnostics of Diabatic Processes, 23-25 April 1986. ECMWF, Reading, 85-99.

Klemp, J.B. and D.K. Lilly, 1980: Mountain waves and momentum flux. GARP publication series No. 23: Orographic Effects in Planetary Flows. World Meteor. Org., Geneva.

Kung, E.C., 1967: Diurnal and long-term variations of the kinetic energy generation and dissipation for a five-year period. Mon.Wea.Rev., 95, 593-606.

Kung, E.C. and W.E. Baker, 1975: Energy transformations in middle-latitude disturbances. Quart.J.Roy.Met.Soc., 101, 793-815.

Lettau, H., 1950: A re-examination of the Leipzig wind profile considering some relations between wind and turbulence in the frictional layer. Tellus, 2, 125-129.

Louis, J.-F., 1979: A parametric model of vertical eddy fluxes in the atmosphere. Bound.Lay.Meteor., 17, 187-202.

Louis, J.-F., M. Tiedtke und J.-F. Geleyn, 1981: A short history of the operational PBL parameterisation at ECWMF. Workshop on Planetary Boundary Layer Parameterization, ECMWF, Reading, 59-79.

Mailhot, J. and R. Benoit, 1982: A finite-element model of the atmospheric boundary layer suitable for use with numerical weather prediction models. J.Atm.Sci., 39, 2249-2266.

Manton, M.J., 1983: On the paramterisation of vertical diffusion in large-scale atmospheric models. ECMWF Tech. Rep. 39, 34 pp.

Melgarejo, J., 1980: A numerical simulation of wind over Gotland with a two-dimensional meso-meteorological boundary layer model. FOU Notiser No. 11. Swedish Meteorological and Hydrological Institute.

Mellor, G.L., 1973: Analytic prediction of the properties of stratified planetary surface layers. J.Atm.Sci., 30, 1061-1069.

Mellor, G.L. and T. Yamada, 1974: A hierarchy of turbulence closure models for planetary boundary layers. J.Atm.Sci., 31, 1791-1806.

Mildner, P., 1932: Über die Reibung in einer speziellen Luftmasse in den untersten Schichten der Atmosphäre. Beitr.Phys.Atmos., 19, 151-158.

Miyakoda, K. and J. Sirutis, 1977: Comparative integration of global models with various parameterized processes of subgrid-scale vertical transports: Description of the parameterizations. Beitr.Phys.Atmos., 50, 445-487.

Miyakoda, K., T. Gordon, R. Caverly, W. Stern, J. Sirutis and W. Bourke, 1983: Simulaton of a blocking event in January 1977, Mon.Wea.Rev., 111, 846-869.

Ninomiya, K and T. Akiyama, 1976: Structure and heat energy budget of a mixed layer capped by inversion during the period of polar outbreak over the Kuroshio region. J.Met.Soc.Japan, 54, 160-174.

Richtmeyer, R.D. and K.W. Morton, 1967: Difference methods for initial-value problems. Interscience, 405pp.

Rodi, W., 1980: Turbulence models and their application in hydraulics. IAHR Publications, Delft, Netherlands.

Rotta, J., 1951: Statistische Theorie nichthomogener Turbulenz. Z.f. Physik, 129, 577-582.

Sommeria, G., 1976: Three-dimensional simulation of turbulent processes in an undisturbed trade wind boundary layer. J.Atm.Sci., 33, 216-241.

Therry, G. and P. Lacarrere, 1983: Improving the eddy-kinetic energy model for planetary boundary layer description. Bound.Lay.Met., 25, 63-88.

Tiedtke, M., 1981: Assessment of the PBL-flow in the EC model. Workshop on Planetary Boundary Layer Parameterization, ECMWF, Reading, 155-191.

Tiedtke,M., J.-F. Geleyn, A, Hollingsworth und J.-F. Louis, 1979: ECMWF model. Parameterization of subgrid scale processes. ECMWF Tech.Rep. 10, 46 pp.

Trout, D. and H.A. Panofsky, 1969: Energy dissipation near the tropopause Tellus, 21, 355-358.

Wyngaard, J.C. and O.R. Cote, 1974: The evolution of a convective planetary boundary layer - a higher order closure model study. Bound.Lay.Meteor., 7, 289-308.

Yamada, T and G.L. Mellor, 1975: A simulation of the Wangara atmospheric boundary layer data. J.Atm.Sci., 32, 2309-2329.

Yamada, T. and G.L. Mellor, 1979: A numerical simulation of BOMEX data using a turbulence closure model coupled with ensemble cloud relations. Quart.J.Roy.Met.Soc., 105, 915-944.